GEOMETRIZED VACUUM PHYSICS. PART 14: "THE HYDROGEN ATOM"

Mikhail Batanov-Gaukhman[1],

(1) Moscow Aviation Institute (National Research University),
Institute № 2 "Aircraft and rocket engines and power plants",
st. Volokolamsk highway, 4, Moscow – Russia, 125993
(e-mail: alsignat@yandex.ru)

2026.06.26

ABSTRACT

This article is the fourteenth part of the scientific project under the general title "Geometrized Vacuum Physics Based on the Algebra of Signature" (GVPh&AS) [1,2,3,4,5,6,7,8,9,10,11,12,13]. In this article, the stochastic metric-dynamic model (SMDM) of the "hydrogen atom" is considered, constructed on the basis of the principles and mathematical apparatus of GVPh&AS. A similar methodology can be applied to study the internal structure of all known "atoms" and "molecules" of both the picoscopic level of matter organization ($\sim 10^{-11} - 10^{-14}$cm), and other levels: microscopic, planetary, galactic, etc. A stochastic Schrödinger equation for the "hydrogen atom" with effective potentiality is proposed, which may allow for a refinement of the fine structure of the emission spectrum of this stable vacuum formation without the use of radiative corrections. A distinctive feature of the SMDM from the quantum mechanical approach (in the Copenhagen interpretation) is that the mathematics of the GVPh&AS allows for the creation of a visual simulation of intra-atomic processes in a form convenient for our perception, i.e., as if peering inside the "atom" and mentally observing the cosmic grandeur of the processes occurring there.

Keywords: vacuum physics, hydrogen atom, stochastic quantum mechanics, stable vacuum formations, Algebra of signature.

BACKGROUND & INTRODUCTION

This is the fourteenth part of a series of articles entitled "Geometrized Vacuum Physics (GVPh) Based on the Algebra of Signature (AS)" (GVPh&AS). The previous thirteen articles are listed in the bibliography [1,2,3,4,5,6,7,8,9,10,11,12,13] and posted on the website https://metraphysics.ru/.

This part of the project aims to examine in more detail the stochastic metric-dynamic model of the "hydrogen atom"* based on the mathematical apparatus of GVPh&AS, developed in the previous articles.

On the one hand, the hydrogen atom is the simplest atom and therefore easier to describe mathematically. On the other hand, the study of the hydrogen atom has left a significant mark on the history of science. Quantum mechanics received its main impetus for development precisely when, in 1925 – 1926, Werner Heisenberg (a student and follower of Niels Bohr) explained the spectrum of its radiation using matrix mechanics, and independently of him, Erwin Schrödinger calculated the hydrogen atom using wave mechanics.

This article, using the example of a stochastic metric-dynamic model of the "hydrogen atom," demonstrates how a model of any "atom" from D.I. Mendeleev's periodic table of chemical elements can be constructed (or, more accurately, visualized).

**Visualized models of picoscopic, on-average, stable spherical vacuum formations ("corpuscles"* or topological knots) with nuclear radii of the order of $r_c \sim 10^{-11} - 10^{-14}$cm differ from the models of elementary particles in modern quantum physics. In GVPh&AS, "corpuscles" are understood to be stable spherical vacuum formations, which are divided into four main parts (see Figures 1 and 2): the outer shell, the core, the raqiya (a spherical chasm of cracks separating the nucleus from the outer shell), and the inner nucleolus. Therefore, within the framework of the GVPh&AS, the names of stable vacuum entities ("corpuscles") are enclosed in quotation marks, for example, "electron," "proton," "neutron," "atom," etc.*

For ease of reference, we present the basic information from the previous sections of the GVPh&AS [1,2,3,4,5,6,7,8,9,10, 11,12,13], which will be needed for the subject of this article.

1. Metric-dynamic models of "quarks" and "antiquarks"

First of all, let us recall that according to the GVPh&AS (see §4.2 in [6]), all picoscopic topological nodes, i.e., elementary "particles," "atoms," and "molecules," consist of colored "quarks" and "antiquarks" with the signatures presented in Table 1.

Table 1 – Signatures of colored "quarks" and "antiquarks" (repeat of Table 1 in [6])

Signature type, i.e. number of + and –	**"Quarks$_k$"**		**"Antiquarks$_k$"**		Color **"quark$_k$"** or **"antiquark$_k$"**
	10 metrics of the type (1) with signature:	Designation **"quark$_k$"**	10 metrics of the type (1)	Designation **"antiquark$_k$"**	
1–3	(+ – – –)	**e_y^+-"quark$_k$"** **(or "electron$_k$")**	(– + + +)	**e_y^--"antiquark$_k$"** **(or "positron$_k$")**	**yellow**
1–3	(+ + + –)	**d_r^+-"quark$_k$"**	(– – – +)	**d_r^--"antiquark$_k$"**	**red**
	(+ + – +)	**d_g^+-"quark$_k$"**	(– – + –)	**d_g^--"antiquark$_k$"**	**green**
	(+ – + +)	**d_b^+-"quark$_k$"**	(– + – –)	**d_b^--"antiquark$_k$"**	**blue**
2–2	(+ – – +)	**u_r^+-"quark$_k$"**	(– + + –)	**u_r^--"antiquark$_k$"**	**red**
	(+ – + –)	**u_g^+-"quark$_k$"**	(– + – +)	**u_g^--"antiquark$_k$"**	**green**
	(+ + – –)	**u_b^+-"quark$_k$"**	(– – + +)	**u_b^--"antiquark$_k$"**	**blue**
4	(+ + + +)	**i_w^+-"quark$_k$"**	(– – – –)	**i_w^--"antiquark$_k$"**	**white**

where the index k in the name "quark" or "antiquark" depends on the number of "corpuscles" in the hierarchical chain of which the given vacuum formation is a part (see [6,10,12]). Within the framework of the 10-level hierarchical cosmological model developed here, this index can take values k = 4,5,6,7,8,9,10. However, to simplify the notation in this article, we will omit the index k, since the location of the picoscopic "corpuscles" in the hierarchical chain has no significant significance with respect to the issues considered in this article.

The metric-dynamic models of 16 picoscopic "quarks" and "antiquarks" are defined by sets of 10 metrics of the (50) or (60) type in [6], but with the corresponding signature from Table 1. As an example, we present the metric-dynamic model of the u_r^--"antiquark" with the signature (or topology) (– + + –) in expanded form:

u_r^--"ANTIQUARK$_k$" (1)

an unstable "convex-concave" vacuum state with signature (– + + –), consisting of:

The outer shell of the u_r^--"antiquark$_k$"

in the interval [r_1, r_6], signature (– + + –)

I $$ds_1^{(-++-)2} = -\left(1 - \frac{r_{6,1}}{r} + \frac{r^2}{r_L^2}\right)c^2dt^2 + \frac{dr^2}{\left(1 - \frac{r_{6,1}}{r} + \frac{r^2}{r_L^2}\right)} + r^2d\theta^2 - r^2\sin^2\theta\, d\phi^2, \quad (2)$$

H $$ds_2^{(-++-)2} = -\left(1 + \frac{r_{6,2}}{r} - \frac{r^2}{r_L^2}\right)c^2dt^2 + \frac{dr^2}{\left(1 + \frac{r_{6,2}}{r} - \frac{r^2}{r_L^2}\right)} + r^2d\theta^2 - r^2\sin^2\theta\, d\phi^2, \quad (3)$$

V $$ds_3^{(-++-)2} = -\left(1 - \frac{r_{6,3}}{r} - \frac{r^2}{r_L^2}\right)c^2dt^2 + \frac{dr^2}{\left(1 - \frac{r_{6,3}}{r} - \frac{r^2}{r_L^2}\right)} + r^2d\theta^2 - r^2\sin^2\theta\, d\phi^2, \quad (4)$$

H′ $$ds_4^{(-++-)2} = -\left(1+\frac{r_{6,4}}{r}+\frac{r^2}{r_L^2}\right)c^2dt^2 + \frac{dr^2}{\left(1+\frac{r_{6,4}}{r}+\frac{r^2}{r_L^2}\right)} + r^2d\theta^2 - r^2 sin^2\theta\, d\phi^2; \quad (5)$$

The core of the u_r^--"antiquark"

in the interval [r_6, r_9], signature (– + + –)

I $$ds_1^{(-++-)2} = -\left(1+\frac{r_S}{r}-\frac{r^2}{r_{6,1}^2}\right)c^2dt^2 + \frac{dr^2}{\left(1+\frac{r_S}{r}-\frac{r^2}{r_{6,1}^2}\right)} + r^2d\theta^2 - r^2 sin^2\theta\, d\phi^2, \quad (6)$$

H $$ds_2^{(-++-)2} = -\left(1-\frac{r_S}{r}+\frac{r^2}{r_{6,2}^2}\right)c^2dt^2 + \frac{dr^2}{\left(1-\frac{r_S}{r}+\frac{r^2}{r_{6,2}^2}\right)} + r^2d\theta^2 - r^2 sin^2\theta\, d\phi^2, \quad (7)$$

V $$ds_3^{(-++-)2} = -\left(1+\frac{r_S}{r}+\frac{r^2}{r_{6,3}^2}\right)c^2dt^2 + \frac{dr^2}{\left(1+\frac{r_S}{r}-\frac{r^2}{r_{6,3}^2}\right)} + r^2d\theta^2 - r^2 sin^2\theta\, d\phi^2, \quad (8)$$

H′ $$ds_4^{(-++-)2} = -\left(1-\frac{r_S}{r}-\frac{r^2}{r_{6,4}^2}\right)c^2dt^2 - \frac{dr^2}{\left(1-\frac{r_S}{r}-\frac{r^2}{r_{6,4}^2}\right)} + r^2d\theta^2 - r^2 sin^2\theta\, d\phi^2; \quad (9)$$

The substrate of the u_r^--"antiquark"

in the interval [0, ∞], signature (– + + –)

i $$ds_5^{(-++-)2} = -c^2dt^2 + dr^2 + r^2d\theta^2 - r^2 \sin^2\theta\, d\phi^2. \quad (10)$$

where, according to the radius hierarchy (44a) in [6]:
$r_{6,1} \approx r_{6,2} \approx r_{6,3} \approx r_{6,4} \approx 10^{-13}$ cm is the radius of the core of an "elementary particle" (in particular, a core of an "electron");
$r_S \approx r_7 \sim 10^{-24}$ cm* is the radius commensurate with the radius of the "proto-quark" nucleolus;
$r_L \approx r_5 \sim 10^{-3}$ cm is the radius commensurate with the radius of a biological "cell".

* *The radius of the proto-quark nucleolus, $r_7 \sim 10^{-24}$ cm, has not been experimentally confirmed. This value was obtained from the heuristic recurrence formula (44) in [6]. Experiments on electron scattering by atoms allow us to confidently assume that $r_7 \ll 10^{-17}$ cm. However, at this stage of research, the exact size of the proto-quark nucleolus is not of great importance. If this value is refined over time, this circumstance will not affect the main aspects of the theory developed in this article.*

The metric-dynamic models of all the remaining 15 "quarks" and "antiquarks" are analogous to the set of 10 metrics (2) – (10), but with the signatures presented in Table 1.

2. The metric-dynamic model of the "electron" (or e_y^+-"quark")

Within the framework of the GVPh&AS developed here, the metric-dynamic model of the "electron" at rest (or e_y^+-"quark", according to the classification given in Table 1) is defined by 10 metric solutions of Einstein's second vacuum equation $R_{im} + g_{im}\Lambda_e = 0$ with signature (+ – – –) (see §4.1 in [6]):

"ELECTRON"

(or e_y^+-"quark") (11)

is, on average, a spherical, stable, convex, multilayered vacuum curvature with a signature (+ – – –), consisting of:

The outer shell of the "electron"

in the interval [r_1,r_6] (Figure 1a), with a signature (+ – – –)

I $$ds_1^{(+---)2} = \left(1-\frac{r_{6,1}}{r}+\frac{r^2}{r_L^2}\right)c^2dt^2 - \frac{dr^2}{\left(1-\frac{r_{6,1}}{r}+\frac{r^2}{r_L^2}\right)} - r^2(d\theta^2 + sin^2\theta\, d\phi^2), \quad (12)$$

H $$ds_2^{(+---)2} = \left(1+\frac{r_{6,2}}{r}-\frac{r^2}{r_L^2}\right)c^2dt^2 - \frac{dr^2}{\left(1+\frac{r_{6,2}}{r}-\frac{r^2}{r_L^2}\right)} - r^2(d\theta^2 + sin^2\theta\, d\phi^2), \quad (13)$$

V $$ds_3^{(+---)2} = \left(1-\frac{r_{6,3},}{r}-\frac{r^2}{r_L^2}\right)c^2dt^2 - \frac{dr^2}{\left(1-\frac{r_{6,3}}{r}-\frac{r^2}{r_L^2}\right)} - r^2(d\theta^2 + sin^2\theta\, d\phi^2), \quad (14)$$

H′ $$ds_4^{(+---)2} = \left(1+\frac{r_{6,4}}{r}+\frac{r^2}{r_L^2}\right)c^2dt^2 - \frac{dr^2}{\left(1+\frac{r_{6,4}}{r}+\frac{r^2}{r_L^2}\right)} - r^2(d\theta^2 + sin^2\theta\, d\phi^2); \quad (15)$$

The "electron's" core

in the interval $[r_6, r_9]$ (Figure 1a), with the signature $(+---)$

I $$ds_1^{(+---)2} = \left(1 + \frac{r_S}{r} - \frac{r^2}{r_{6,1}^2}\right)c^2dt^2 - \frac{dr^2}{\left(1 + \frac{r_S}{r} - \frac{r^2}{r_{6,1}^2}\right)} - r^2(d\theta^2 + \sin^2\theta\, d\phi^2), \quad (16)$$

H $$ds_2^{(+---)2} = \left(1 - \frac{r_S}{r} + \frac{r^2}{r_{6,2}^2}\right)c^2dt^2 - \frac{dr^2}{\left(1 - \frac{r_S}{r} + \frac{r^2}{r_{6,2}^2}\right)} - r^2(d\theta^2 + \sin^2\theta\, d\phi^2), \quad (17)$$

V $$ds_3^{(+---)2} = \left(1 + \frac{r_S}{r} + \frac{r^2}{r_{6,3}^2}\right)c^2dt^2 - \frac{dr^2}{\left(1 + \frac{r_S}{r} - \frac{r^2}{r_{6,3}^2}\right)} - r^2(d\theta^2 + \sin^2\theta\, d\phi^2), \quad (18)$$

H′ $$ds_4^{(+---)2} = \left(1 - \frac{r_S}{r} - \frac{r^2}{r_{6,4}^2}\right)c^2dt^2 - \frac{dr^2}{\left(1 - \frac{r_S}{r} - \frac{r^2}{r_{6,4}^2}\right)} - r^2(d\theta^2 + \sin^2\theta\, d\phi^2); \quad (19)$$

The substrate of the "electron"

in the interval $[0, \infty]$, signature $(+---)$

i $$ds_5^{(+---)2} = c^2dt^2 - dr^2 - r^2(d\theta^2 + \sin^2\theta\, d\phi^2), \quad (20)$$

Based on the analysis of a set of metrics of the form (12) – (20) using GVPh&AS methods in [7], a visualized model of the "electron" (i.e., the yellow e_y^+-"quark") was obtained, shown in Figure1 (repetition of Figure 1 in [7]). Thus, within the framework of GVPh&AS, a resting "electron" is, on average, a convex spherical vacuum formation, which occupies the entire volume of the previous spherical vacuum formation in which it is located (for example, the entire interior of a "biological cell", or the entire core of a "planet", or the entire closed "Universe", see §2.1 in [7]). Inside the "electron" there is a clearly defined average core with a radius of the order of $r_6 \sim 10^{-13}$cm, while inside this core there is a tiny nucleolus (like a seed inside an apple), this is the nucleolus of an e_y^+-"proto-quark" with a characteristic radius of the order of $r_7 \sim 10^{-24}$cm. Later, however, it will become clear that inside the core of the "electron" there may be not one, but many "proto-quark's" nuclei.

Later, it will become clear that within the "electron's" core there may be not one, but many averaged virtual "proto-quark" nucleoli. That is, upon closer examination, within the "electron" core there may be one or more valence tiny nucleoli and many virtual tiny nucleoli. This is similar to a biological cell, which may have one or two nuclei and many other organelles (mitochondria, ribosomes, lysosomes, etc.). It has previously been noted in the GVF&AS that "elementary particles" (in particular, "electrons" and "positrons," "protons" and "neutrons," and "atoms") can be considered the physical shells of the Fermi bacteria and Fermi viruses.

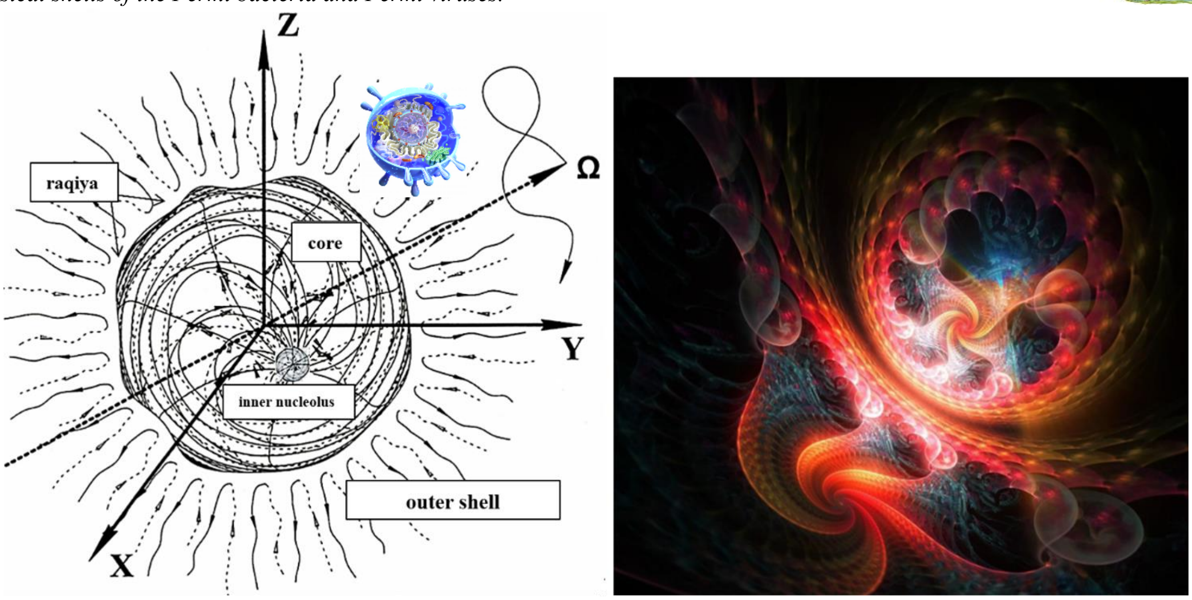

a) b)

Fig. 1: (repeat of Figure 1 in [7]) Illustration of a stochastic metric-dynamic model of a stable spherical vacuum formation (a "corpuscle," in particular, an "electron"), in the vicinity of its nucleus with four clearly defined regions:

The core of the "corpuscle" (in particular, of the "electron's" core) is a central closed spherical (on average) region of vacuum with a characteristic radius from hierarchy (44a) in [8] $r_6 \sim 10^{-13}$cm, and a complex internal structure;
The inner nucleolus of the "corpuscle" (in particular, of the "electron") is a tiny closed spherical region of vacuum within the nucleus – this is the nucleolus of the "proto-quark" with a characteristic radius $r_7 \sim 10^{-24}$ cm;
The outer shell of the "corpuscle" (in particular, of the "electron") is a region of vacuum surrounding its core. The outer shell of a "corpuscle" extends from its core to the inner boundaries of the significantly larger core of the next-largest "corpuscle" (for example, from the core of an "electron" to the inner boundary of the nucleus of a "biological cell"), within which this core is located (Figs. 1 and 10 in [6]);
The raqiya of a "corpuscle" (in particular, of an "electron") is a multilayered spherical abyss-crack separating the core of the "corpuscle" from its outer shell (see §4.11 in [6]);
The substrate of a "corpuscle" is a kind of memory of the initial, undeformed state of the vacuum region in which the "corpuscle" is located. That is, this is the initial vacuum region, before it was deformed and assumed the stable shape of a convex "corpuscle" or a concave "anticorpuscle," in particular, of an "electron" (or "positron").

3. Metric-dynamic model of the "positron" (or yellow e_y^--"antiquark")

Within the framework of the GVPh&AS, the metric-dynamic model of the "positron" at rest (or e_y^--"antiquark" in Table 1) is defined by 10 metric solutions of Einstein's second vacuum equation $R_{im} - g_{im}\Lambda = 0$ of the form (12) – (20), but with the opposite signature (– + + +) (see §4.11 in [6]):

"POSITRON" (21)

(or $\mathbf{e}_y^-$-"antiquark")

is, on average, a spherical, stable, concave, multilayered

vacuum curvature with a signature (– + + +), consisting of:

The outer shell of the "positron"

in the interval $[r_1, r_6]$ (negative of Figure 1a), with a signature (– + + +)

I $$ds_1^{(-+++)2} = -\left(1 - \frac{r_{6,1}}{r} + \frac{r^2}{r_L^2}\right)c^2dt^2 + \frac{dr^2}{\left(1 - \frac{r_{6,1}}{r} + \frac{r^2}{r_L^2}\right)} + r^2(d\theta^2 + \sin^2\theta\, d\phi^2), \quad (22)$$

H $$ds_2^{(-+++)2} = -\left(1 + \frac{r_{6,2}}{r} - \frac{r^2}{r_L^2}\right)c^2dt^2 + \frac{dr^2}{\left(1 + \frac{r_{6,2}}{r} - \frac{r^2}{r_L^2}\right)} + r^2(d\theta^2 + \sin^2\theta\, d\phi^2), \quad (23)$$

V $$ds_3^{(-+++)2} = -\left(1 - \frac{r_{6,3}}{r} - \frac{r^2}{r_L^2}\right)c^2dt^2 + \frac{dr^2}{\left(1 - \frac{r_{6,3}}{r} - \frac{r^2}{r_L^2}\right)} + r^2(d\theta^2 + \sin^2\theta\, d\phi^2), \quad (24)$$

H′ $$ds_4^{(-+++)2} = -\left(1 + \frac{r_{6,4}}{r} + \frac{r^2}{r_L^2}\right)c^2dt^2 + \frac{dr^2}{\left(1 + \frac{r_{6,4}}{r} + \frac{r^2}{r_L^2}\right)} + r^2(d\theta^2 + \sin^2\theta\, d\phi^2); \quad (25)$$

The "positron's" core

in the interval $[r_6, r_9]$ (Figure 1a), with the signature (– + + +)

I $$ds_1^{(-+++)2} = -\left(1 + \frac{r_S}{r} - \frac{r^2}{r_{6,1}^2}\right)c^2dt^2 + \frac{dr^2}{\left(1 + \frac{r_S}{r} - \frac{r^2}{r_{6,1}^2}\right)} + r^2(d\theta^2 + \sin^2\theta\, d\phi^2), \quad (26)$$

H $$ds_2^{(-+++)2} = -\left(1 - \frac{r_S}{r} + \frac{r^2}{r_{6,2}^2}\right)c^2dt^2 + \frac{dr^2}{\left(1 - \frac{r_S}{r} + \frac{r^2}{r_{6,2}^2}\right)} + r^2(d\theta^2 + \sin^2\theta\, d\phi^2), \quad (27)$$

V $$ds_3^{(-+++)2} = -\left(1 + \frac{r_S}{r} + \frac{r^2}{r_{6,3}^2}\right)c^2dt^2 + \frac{dr^2}{\left(1 + \frac{r_S}{r} - \frac{r^2}{r_{6,3}^2}\right)} + r^2(d\theta^2 + \sin^2\theta\, d\phi^2), \quad (28)$$

H′ $$ds_4^{(-+++)2} = -\left(1 - \frac{r_S}{r} - \frac{r^2}{r_{6,4}^2}\right)c^2dt^2 + \frac{dr^2}{\left(1 - \frac{r_S}{r} - \frac{r^2}{r_{6,4}^2}\right)} + r^2(d\theta^2 + \sin^2\theta\, d\phi^2); \quad (29)$$

The substrate of the "positron"

in the interval $[0, \infty]$, signature (– + + +)

i $$ds_5^{(-+++)2} = -c^2dt^2 + dr^2 + r^2(d\theta^2 + \sin^2\theta\, d\phi^2). \quad (30)$$

Within the framework of the concepts developed here, a "positron" is a stable, on average, concave spherical vacuum formation with a picoscopic (~ 10^{-13} cm) core, inside which there is an ioctoscopic (~ 10^{-24} cm) nucleolus of a "proto-antiquark" (negative Figure 1). In other words, a "positron" is, on average, a complete negative copy of an "electron". If we add metrics (12) – (20) with the corresponding metrics (22) – (30), we obtain the initial zero (i.e., the initial uncurved state of a two-sided vacuum, taking into account the vacuum balance condition, see Introduction in [1]).

4. Metric-dynamic models of the "proton" and "antiproton"

In §4.3 of [6], it is shown that stable, on average, spherical vacuum formations can be a set of topological nodes ("corpuscles") with total signatures (+ – – –) or (– + + +). Specifically, such "corpuscles" ("protons" and "antiprotons") can be composed of three different-colored "quarks" and "antiquarks" from Table 1:

$$
\begin{array}{lclclc}
\boldsymbol{d}_r^{+}(+\ +\ +\ -) & & \boldsymbol{d}_g^{+}(+\ +\ -\ +) & & \boldsymbol{d}_b^{+}(+\ -\ +\ +) & \\
\boldsymbol{u}_g^{-}(-\ +\ -\ +) & (31) & \boldsymbol{u}_b^{-}(-\ -\ +\ +) & (32) & \boldsymbol{u}_r^{-}(-\ +\ +\ -) & (33) \\
\boldsymbol{u}_b^{-}\underline{(-\ -\ +\ +)} & & \boldsymbol{u}_r^{-}\underline{(-\ +\ +\ -)} & & \boldsymbol{u}_g^{-}\underline{(-\ +\ -\ +)} & \\
\boldsymbol{p}_1^{-}(-\ +\ +\ +)_+ & & \boldsymbol{p}_2^{-}(-\ +\ +\ +)_+ & & \boldsymbol{p}_3^{-}(-\ +\ +\ +)_+ &
\end{array}
$$

where p_i^- are three possible states of the p_i^--“proton” ($\underline{i}$ = 1,2,3) with the signature (– + + +).

$$
\begin{array}{lclclc}
\boldsymbol{d}_r^{-}(-\ -\ -\ +) & & \boldsymbol{d}_g^{-}(-\ -\ +\ -) & & \boldsymbol{d}_r^{-}(-\ +\ -\ -) & \\
\boldsymbol{u}_g^{+}(+\ -\ +\ -) & (34) & \boldsymbol{u}_b^{+}(+\ +\ -\ -) & (35) & \boldsymbol{u}_b^{+}(+\ -\ -\ +) & (36) \\
\boldsymbol{u}_b^{+}\underline{(+\ +\ -\ -)} & & \boldsymbol{u}_r^{+}\underline{(+\ -\ -\ +)} & & \boldsymbol{u}_g^{+}\underline{(+\ -\ +\ -)} & \\
\boldsymbol{p}_1^{+}(+\ -\ -\ -)_+ & & \boldsymbol{p}_2^{+}(+\ -\ -\ -)_+ & & \boldsymbol{p}_3^{+}(+\ -\ -\ -)_+ &
\end{array}
$$

where p_i^+ are three possible states of the p_i^+-“antiproton” with the signature (+ – – –).

Each signature in the rankings (31) – (36) corresponds to a topology of a 4-dimensional subspace (see §4 in [2]), so these signature combinations can also be called topological nodes.

Recall that, within the framework of the GVPh&AS, each signature in the rankings (31) – (33) corresponds to a "quark" or "anti-quark" from Table 1, the metric-dynamic model of which is determined by 10 metrics of the form (2) – (10) or (12) – (20) or (22) – (30), but with the corresponding signature.

In a more compact form, the states of the p_i^--"proton" and p_i^+- antiproton" can be written as is customary in quantum chromo-dynamics.

$$p_1^- = u_g^- u_b^- d_r^+, \quad p_2^- = u_r^- u_b^- d_g^+, \quad p_3^- = u_g^- u_r^- d_b^+, \tag{37}$$

$$p_1^+ = u_g^+ u_b^+ d_r^-, \quad p_2^+ = u_r^+ u_b^+ d_g^-, \quad p_3^+ = u_g^+ u_r^+ d_b^-. \tag{38}$$

Unlike quantum chromodynamics, where protons consist of *d* and u quarks, in quantum physics, in GVPh&AS a "proton" consists of a d_i^+-"quark" and two u_J^--"antiquarks." Recall that a "quark" or "antiquark" is determined by the first sign in the signature: (+) corresponds to a "quark," (–) corresponds to an "antiquark." This first sign in the signature determines the direction of the vacuum sheath flow and ultimately corresponds to the "charge" of the vacuum structure (see [4] and §2.2 in [7]). Let us recall that in the GVPh&AS there is no problem of baryon asymmetry of matter (see [6]), since within the framework of this theory "matter" and "antimatter" are mixed with each other. They don't annihilate due to constant thermal motion (mixing). Therefore, within the framework of the GVPh&AS, the world exists in particulars, but in general (i.e., on average), this world does not exist.

For example, imagine the topological node (31) (i.e., p_1^--“proton”)

$$
\begin{array}{l}
\boldsymbol{d}_r^{+}(+\ +\ +\ -) \\
\boldsymbol{u}_g^{-}(-\ +\ -\ +) \\
\boldsymbol{u}_b^{-}\underline{(-\ -\ +\ +)} \\
\boldsymbol{p}_1^{-}(-\ +\ +\ +)_+
\end{array}
$$

in expanded form (see (92) in [6]):

P_1^--"PROTON" (39)

is a stable, on average, concave spherical vacuum formation with a common signature (– + + +), consisting of one colored d_i^+-"quark" and two colored u_J^--"antiquarks":

d_r^+-"quark"

a convex-concave vacuum formation with the signature (+ + + –), consisting of:

The outer shell of the d_r^+-"quark" (40)

in the interval $[r_5, r_6]$ (Figure 2), signature (+ + + –)

$$ds_1^{(+++-)2} = \left(1 - \frac{r_6}{r} + \frac{r^2}{r_L^2}\right) c^2 dt^2 + \frac{dr^2}{\left(1 - \frac{r_6}{r} + \frac{r^2}{r_L^2}\right)} + r^2 d\theta^2 - r^2 \sin^2\theta\, d\phi^2,$$

$$ds_2^{(+++-)2} = \left(1 + \frac{r_6}{r} - \frac{r^2}{r_L^2}\right) c^2 dt^2 + \frac{dr^2}{\left(1 + \frac{r_6}{r} - \frac{r^2}{r_L^2}\right)} + r^2 d\theta^2 - r^2 \sin^2\theta\, d\phi^2,$$

$$ds_3^{(+++-)2} = \left(1 - \frac{r_6}{r} - \frac{r^2}{r_L^2}\right) c^2 dt^2 + \frac{dr^2}{\left(1 - \frac{r_6}{r} - \frac{r^2}{r_L^2}\right)} + r^2 d\theta^2 - r^2 \sin^2\theta\, d\phi^2,$$

$$ds_4^{(+++-)2} = \left(1 + \frac{r_6}{r} + \frac{r^2}{r_L^2}\right) c^2 dt^2 + \frac{dr^2}{\left(1 + \frac{r_6}{r} + \frac{r^2}{r_L^2}\right)} + r^2 d\theta^2 - r^2 \sin^2\theta\, d\phi^2$$

The d_r^+-"quark's"core (41)

in the interval $[r_6, r_9]$ (Figure 2), with the signature (+ + + –)

$$ds_1^{(+++-)2} = \left(1 - \frac{r_S}{r} + \frac{r^2}{r_{6,1}^2}\right) c^2 dt^2 + \frac{dr^2}{\left(1 - \frac{r_S}{r} + \frac{r^2}{r_{6,1}^2}\right)} + r^2 d\theta^2 - r^2 \sin^2\theta\, d\phi^2,$$

$$ds_2^{(+++-)2} = \left(1 + \frac{r_S}{r} - \frac{r^2}{r_{6,2}^2}\right) c^2 dt^2 + \frac{dr^2}{\left(1 + \frac{r_S}{r} - \frac{r^2}{r_{6,2}^2}\right)} + r^2 d\theta^2 - r^2 \sin^2\theta\, d\phi^2,$$

$$ds_3^{(+++-)2} = \left(1 - \frac{r_S}{r} - \frac{r^2}{r_{6,3}^2}\right) c^2 dt^2 + \frac{dr^2}{\left(1 - \frac{r_S}{r} - \frac{r^2}{r_{6,3}^2}\right)} + r^2 d\theta^2 - r^2 \sin^2\theta\, d\phi^2,$$

$$ds_4^{(+++-)2} = \left(1 + \frac{r_S}{r} + \frac{r^2}{r_{6,4}^2}\right) c^2 dt^2 + \frac{dr^2}{\left(1 + \frac{r_S}{r} + \frac{r^2}{r_{6,5}^2}\right)} + r^2 d\theta^2 - r^2 \sin^2\theta\, d\phi^2;$$

The substrate of the d_r^+-"quark"

in the interval $[0, \infty]$, signature (+ + + –)

$$ds_5^{(+++-)2} = c^2 dt^2 + dr^2 + r^2 d\theta^2 - r^2 \sin^2\theta\, d\phi^2.$$

u_g^-- "antiquark"

a concave-convex vacuum formation with the signature (– + – +), consisting of:

The outer shell of the u_g^--"antiquark" (43)

in the interval $[r_5, r_6]$ (Figure 2), signature (– + – +)

$$ds_1^{(-+-+)2} = -\left(1 - \frac{r_{6,1}}{r} + \frac{r^2}{r_L^2}\right) c^2 dt^2 + \frac{dr^2}{\left(1 - \frac{r_{6,1}}{r} + \frac{r^2}{r_L^2}\right)} - r^2 d\theta^2 + r^2 \sin^2\theta\, d\phi^2,$$

$$ds_2^{(-+-+)2} = -\left(1 + \frac{r_{6,2}}{r} - \frac{r^2}{r_L^2}\right) c^2 dt^2 + \frac{dr^2}{\left(1 + \frac{r_{6,2}}{r} - \frac{r^2}{r_L^2}\right)} - r^2 d\theta^2 + r^2 \sin^2\theta\, d\phi^2,$$

$$ds_3^{(-+-+)2} = -\left(1 - \frac{r_{6,3}}{r} - \frac{r^2}{r_L^2}\right) c^2 dt^2 + \frac{dr^2}{\left(1 - \frac{r_{6,3}}{r} - \frac{r^2}{r_L^2}\right)} - r^2 d\theta^2 + r^2 \sin^2\theta\, d\phi^2,$$

$$ds_4^{(-+-+)2} = -\left(1 + \frac{r_{6,4}}{r} + \frac{r^2}{r_L^2}\right) c^2 dt^2 + \frac{dr^2}{\left(1 + \frac{r_{6,4}}{r} + \frac{r^2}{r_L^2}\right)} - r^2 d\theta^2 + r^2 \sin^2\theta\, d\phi^2;$$

The u_g^--"antiquark's" core (44)

in the interval $[r_6, r_9]$ (Figure 2), with the signature (– + – +)

$$ds_1^{(-+-+)2} = -\left(1 - \frac{r_S}{r} + \frac{r^2}{r_{6,1}^2}\right) c^2 dt^2 + \frac{dr^2}{\left(1 - \frac{r_S}{r} + \frac{r^2}{r_{6,1}^2}\right)} - r^2 d\theta^2 + r^2 \sin^2\theta\, d\phi^2,$$

$$ds_2^{(-+-+)2} = -\left(1+\frac{r_S}{r}-\frac{r^2}{r_{6,2}^2}\right)c^2dt^2 + \frac{dr^2}{\left(1+\frac{r_S}{r}-\frac{r^2}{r_{6,2}^2}\right)} - r^2d\theta^2 + r^2\sin^2\theta\, d\phi^2,$$

$$ds_3^{(-+-+)2} = -\left(1-\frac{r_S}{r}-\frac{r^2}{r_{6,3}^2}\right)c^2dt^2 + \frac{dr^2}{\left(1-\frac{r_S}{r}-\frac{r^2}{r_{6,3}^2}\right)} - r^2d\theta^2 + r^2\sin^2\theta\, d\phi^2,$$

$$ds_4^{(-+-+)2} = -\left(1+\frac{r_S}{r}+\frac{r^2}{r_{6,4}^2}\right)c^2dt^2 + \frac{dr^2}{\left(1+\frac{r_S}{r}+\frac{r^2}{r_{6,4}^2}\right)} - r^2d\theta^2 + r^2\sin^2\theta\, d\phi^2;$$

The substrate of the u_g^--"antiquark"

in the interval [0, ∞], signature (– + – +)

$$ds_5^{(-+-+)2} = -c^2dt^2 + dr^2 - r^2d\theta^2 + r^2\sin^2\theta\, d\phi^2. \quad (45)$$

u_b^-- "antiquark"

a concave-convex vacuum formation with the signature (– – + +), consisting of:

The outer shell of the u_b^--"antiquark" (46)

in the interval [r_5,r_6] (Figure 2), signature (– – + +)

$$ds_1^{(--++)2} = -\left(1-\frac{r_{6,1}}{r}+\frac{r^2}{r_L^2}\right)c^2dt^2 - \frac{dr^2}{\left(1-\frac{r_{6,1}}{r}+\frac{r^2}{r_L^2}\right)} + r^2d\theta^2 + r^2\sin^2\theta\, d\phi^2,$$

$$ds_2^{(--++)2} = -\left(1+\frac{r_{6,2}}{r}-\frac{r^2}{r_L^2}\right)c^2dt^2 - \frac{dr^2}{\left(1+\frac{r_{6,2}}{r}-\frac{r^2}{r_L^2}\right)} + r^2d\theta^2 + r^2\sin^2\theta\, d\phi^2,$$

$$ds_3^{(--++)2} = -\left(1-\frac{r_{6,3}}{r}-\frac{r^2}{r_L^2}\right)c^2dt^2 - \frac{dr^2}{\left(1-\frac{r_{6,3}}{r}-\frac{r^2}{r_L^2}\right)} + r^2d\theta^2 + r^2\sin^2\theta\, d\phi^2,$$

$$ds_4^{(--++)2} = -\left(1+\frac{r_{6,4}}{r}+\frac{r^2}{r_L^2}\right)c^2dt^2 - \frac{dr^2}{\left(1+\frac{r_{6,4}}{r}+\frac{r^2}{L}\right)} + r^2d\theta^2 + r^2\sin^2\theta\, d\phi^2;$$

The u_b^--"antiquark's" core

in the interval [r_6,r_9] (Figure 2), with the signature (– – + +) (47)

$$ds_1^{(--++)2} = -\left(1-\frac{r_S}{r}+\frac{r^2}{r_{6,1}^2}\right)c^2dt^2 - \frac{dr^2}{\left(1-\frac{r_S}{r}+\frac{r^2}{r_{6,1}^2}\right)} + r^2d\theta^2 + r^2\sin^2\theta\, d\phi^2,$$

$$ds_2^{(--++)2} = -\left(1+\frac{r_S}{r}-\frac{r^2}{r_{6,2}^2}\right)c^2dt^2 - \frac{dr^2}{\left(1+\frac{r_S}{r}-\frac{r^2}{r_{6,2}^2}\right)} + r^2d\theta^2 + r^2\sin^2\theta\, d\phi^2,$$

$$ds_3^{(--++)2} = -\left(1-\frac{r_S}{r}-\frac{r^2}{r_{6,3}^2}\right)c^2dt^2 - \frac{dr^2}{\left(1-\frac{r_S}{r}-\frac{r^2}{r_{6,3}^2}\right)} + r^2d\theta^2 + r^2\sin^2\theta\, d\phi^2,$$

$$ds_4^{(--++)2} = -\left(1+\frac{r_S}{r}+\frac{r^2}{r_{6,4}^2}\right)c^2dt^2 - \frac{dr^2}{\left(1+\frac{r_S}{r}+\frac{r^2}{r_{6,4}^2}\right)} + r^2d\theta^2 + \sin^2\theta\, d\phi^2;$$

The substrate of the u_b^--"antiquark"

in the interval [0, ∞], signature (– – + +)

$$ds_5^{(--++)2} = -c^2dt^2 - dr^2 + r^2d\theta^2 + r^2\sin^2\theta\, d\phi^2. \quad (48)$$

Figure 2 shows a visualization of the stochastic metric-dynamic model of the «proton», consisting of: the core of a resting "proton", its near outer shell, and the inner 1/3-nucleus* d_i^+-"proto-quark" and two u_j^--"proto-antiquarks", chaotically wandering relative to each other and constantly changing the overall topological (signature) configuration. This visualized metric-dynamic model of a resting "proton" is obtained based on the analysis of the set of metrics (40) – (48), carried out using the methods of Geometricized Vacuum Physics Based on the Algebra of Signature (GVPh&AS) [2,3,4,6,7].

**Let us explain what 1/3 nucleoli "proto-quark" and "proto-antiquark" mean. Each of these 1/3 nucleoli is a highly curved convex-concave or concave-convex state of a local vacuum region with a characteristic size of the order of ~ 10^{-24} cm. Separately, they cannot exist for a long time, because do not obey conservation laws, i.e. Einstein's vacuum equations. But they also cannot occupy one volume of space, because each of them strives to occupy the center of the general vacuum formation, and can occupy it on average 1/3 of the time, but then is pushed out of the center by other 1/3 nucleoli. In place, they form 1/3 + 1/3 + 1/3 = one full-fledged nucleolus. But this nucleolus has an expanded, bubbling shape, which can only be considered spherical on average with a characteristic size of the order of ~ 10^{-14} cm. In addition, after approximately every 1/3 of the time, the common nucleolus changes its topological (signature or nodal) configuration, because any of the configurations (31) – (33) has the right to exist with probability 1/3. As a result, the central region of the "proton" core is an extremely complexly curved and bubbling section of vacuum (see Figure 2).*

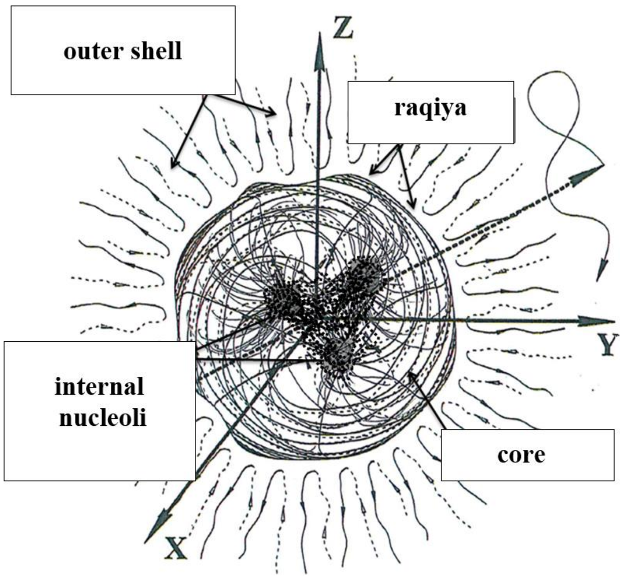


Fig. 2: Visualized stochastic metric-dynamic model of an average concave spherical stable vacuum formation (in particular, a p_i^--"proton"), consisting of 2 colored "antiquarks" and one "quark" (40) – (48). The inner nucleoli (i.e., colored "proto-quarks" and "proto-antiquarks") of these vacuum formations are in constant chaotic movement relative to each other and relative to the common center of the p_i^--"proton's" core

When adding homogeneous terms in metrics (40) – (42), (43) – (45), and (46) – (48) according to the algorithm specified in ranking (31), the resulting set of metrics (22) – (30) describes the metric-dynamic state of the "positron." However, within the "proton's" core, it is necessary to take into account the constant chaotic displacement of the inner nucleolus of the d_r^+-"quark" and the inner nucleoli of the u_g^--"antiquark" and u_b^--"antiquark" relative to each other and relative to the common center $r = 0$ (see Figure 2), and the constant topological rearrangements between the nodal states (31) – (33) (see Figure 6).

That is, the "proton" constantly transitions from a state with one composition of colored "quarks" and "antiquarks" to a state with a different composition through the exchange of "gluons" (136) – (138) in [6]. In other words, the vacuum deformations inside the "proton's" core are constantly being complexly restructured. Therefore, in real time, the average state of the "proton"* is observed.

$$p^- = 1/3\ (p^-_1 + p^-_2 + p^-_3) \tag{49}$$

or taking into account (37):

$$p^- = 1/3\ (\boldsymbol{u_g^- u_b^- d_r^+} + \boldsymbol{u^-_b u_r^- d^+_g} + \boldsymbol{u_g^- u_r^- d_b^+}). \tag{50}$$

*This is one of the differences between the Geometricized Vacuum Physics Based on Algebra of Signature (GVPh&AS) proposed here and Einstein's General Relativity (GR). GVPh&AS takes into account all possible solution metrics of Einstein's vacuum equations or combinations of non-solution metrics like (31) – (36), which, on average, lead to solution metrics. All these solution metrics are considered to partially describe the vacuum structure under study, but in proportion to the probability of this solution's manifestation. Thus, probability theory is woven into GVPh&AS not only because the vacuum fluctuates everywhere, and therefore the mathematical apparatus of modified GR reveals only the averaged states of stable and unstable vacuum structures, but also because the probability of a particular solution of the modified GRA equations participating in the description of the metric-dynamic model of the vacuum structure under study is taken into account.

Similarly, the average state of the "antiproton" is determined by the expression

$$p^+ = 1/3\ (p^+{}_1 + p^+{}_2 + p^+{}_3), \tag{51}$$

or, taking into account (38),

$$p^+ = 1/3\ (u_g^+ u_b^+ d_r^- \ + \ u_b^+ u_r^+ d_g^- \ + \ u_g^+ u_r^+ d_b^-). \tag{52}$$

The set of solution metrics (40) – (48), when using the mathematical apparatus of the GVPh&AS [2,3,4,5,6,7], allows us to extract information about a multitude of processes occurring inside the core of the "proton" and "antiproton", in their raqiyas, and in the outer shells.

5. Metric-dynamic model of the "neutron"

Within the framework of the GVPh&AS developed here, an electrically neutral* "corpuscle" ("neutron") has the following topological (nodal) configurations (see §4.4 in [6]):

$$\begin{array}{lll}
i_w^-\ (-\ -\ -\ -) & i_w^-\ (-\ -\ -\ -) & i_w^-\ (-\ -\ -\ -) \\
d_b^+\ (+\ -\ +\ +)\ \text{(а)} & d_g^+\ (+\ +\ -\ +)\ \text{(б)} & d_b^+\ (+\ -\ +\ +)\ \text{(в)} \\
u_r^-\ (-\ +\ +\ -) & d_r^+\ (+\ +\ +\ -) & u_g^-\ (-\ +\ -\ +) \\
d_g^+\ \underline{(+\ +\ -\ +)} & u_b^-\ \underline{(-\ -\ +\ +)} & d_r^+\ \underline{(+\ +\ +\ -)} \\
n_1^0\ (0\ 0\ 0\ 0)_+ & n_2^0\ (0\ 0\ 0\ 0)_+ & n_3^0\ (0\ 0\ 0\ 0)_+ \\
 & & \\
i_w^+\ (+\ +\ +\ +) & i_w^+\ (+\ +\ +\ +) & i_w^+\ (+\ +\ +\ +) \\
d_b^-\ (-\ +\ -\ -)\ \text{(г)} & d_g^-\ (-\ -\ +\ -)\ \text{(д)} & d_b^-\ (-\ +\ -\ -)\ \text{(е)} \\
u_r^+\ (+\ -\ -\ +) & d_r^-\ (-\ -\ -\ +) & u_g^+\ (+\ -\ +\ -) \\
d_g^-\ \underline{(-\ -\ +\ -)} & u_b^+\ \underline{(+\ +\ -\ -)} & d_r^-\ \underline{(-\ -\ -\ +)} \\
n_4^0\ (0\ 0\ 0\ 0)_+ & n_5^0\ (0\ 0\ 0\ 0)_+ & n_6^0\ (0\ 0\ 0\ 0)_+
\end{array} \tag{53}$$

Each signature in the rankings (53) corresponds to a "quark" or "antiquark" from Table 1, each of which is described by a set of 10 metrics of the form (2) – (10) with the corresponding signature.

**The electrical neutrality of a stable vacuum formation in the GVPh&AS implies that it is, on average, flat (i.e., neither convex nor concave). In the core of such a vacuum formation, a swirling of "proto-quarks" and "proto-antiquarks" occurs, but in the outer shell, all currents and anti-currents, deformations and anti-deformations almost completely cancel each other out. Therefore, neutral vacuum formations interact with other "corpuscles" primarily through the collision of their cores. In other words, there is no electric field around the cores of neutral stable vacuum formations ("corpuscles"). For the electric field geometrization within the GVPh&AS framework, see §4 and 5 in [4], and §2.2.2 in [7]).*

The i_w^+-"quark" and i_w^--"antiquark" are called white because they are practically invisible inside the "neutron's" core, since from a topological point of view, they represent a "point" and an "antipoint" (see §4 in [2]).

The "neutron" states (i.e., the topological nodes (53)) can be represented in a more traditional

$$n_1^0 = i_w^- d_b^+ d_g^+ u_r^-, \quad n_2^0 = i_w^- d_r^+ d_g^+ u_b^-, \quad n_3^0 = i_w^- d_r^+ d_b^+ u_g^-, \tag{54}$$

$$n_4^0 = i_w^+ d_b^- d_g^- u_r^+, \quad n_5^0 = i_w^+ d_r^- d_g^- u_b^+, \quad n_6^0 = i_w^+ d_r^- d_b^- u_g^+.$$

This notation of topological nodes (i.e., "neutron" states) differs from the notation of the neutron's composition in quantum chromodynamics by the presence of invisible i_w^+-"quark" and i_w^--"antiquark."

Due to complex intranuclear topological metamorphoses, any additive 4-"quark"-"antiquark" ranking combination (53) can rearrange itself so that within the core of a given vacuum formation, a p_i–"proton" and an "electron" (i.e., a hydrogen "atom") are obtained:

$$\boxed{\text{"neutron" (53a)}}\quad \begin{array}{c} (-\;-\;-\;-)\\ (+\;-\;+\;+)\\ (-\;+\;+\;-)\\ \underline{(+\;+\;-\;+)}\\ (0\;\;0\;\;0\;\;0)_+ \end{array} \;\longrightarrow\; \begin{array}{c} (+\;-\;+\;+)\\ (-\;+\;+\;-)\\ (-\;+\;-\;+)\\ \underline{(+\;-\;-\;-)}\\ (0\;\;0\;\;0\;\;0)_+ \end{array} \begin{array}{l} \boxed{p_i^-\text{-"proton" (33)}} \\ \\ \boxed{\text{"electron" (11)}} \end{array} \qquad (55)$$

Such a rearrangement (i.e., the re-tying of a topological node) inside the core of a “neutron” can in some cases lead to a decay into a “proton”, “electron” and “neutrino”:

$$n \rightarrow p^- + e^+ + \nu_{e+},$$

where ν_{e+} is an “electron’s neutrino”.

Note that in signature metamorphoses (i.e., in the processes of tying topological nodes), the law of conservation of the signs “+” and “–” operates. For example, in the ranking expression (55) before the transformation there were 8 “+” and 8 “–” and after the transformation there were 8 “+” and 8 “–”.

Intranuclear signature (i.e., topological) transformations can also lead to configurations of “quarks” and “antiquarks” in the form of p_1^+- “antiproton” and “positron” (i.e., “anti-atom” of hydrogen)

$$\boxed{\text{"neutron" (53a)}}\quad \begin{array}{c} (-\;-\;-\;-)\\ (+\;-\;+\;+)\\ (-\;+\;+\;-)\\ \underline{(+\;+\;-\;+)}\\ (0\;\;0\;\;0\;\;0)_+ \end{array} \;\longrightarrow\; \begin{array}{c} (+\;-\;+\;-)\\ (-\;+\;-\;-)\\ (+\;-\;-\;+)\\ \underline{(-\;+\;+\;+)}\\ (0\;\;0\;\;0\;\;0)_+ \end{array} \begin{array}{l} \boxed{p_1^+\text{-“antiproton” (36)}} \\ \\ \boxed{\text{“positron” (21)}} \end{array} \qquad (56)$$

This could lead to the decay of a "neutron" into a p_1^+-"antiproton" and a "positron":

$$n \rightarrow p^+ + e^- + \nu_{e-}, \qquad (57)$$

where ν_{e+} is the "positron’s neutrino".

Such decays should be detected in practice. If this prediction of the GVPh&AS is not confirmed, then the reason for the absence of decays of type (57) must be sought.

One such reason could be the following: in the case of a neutron transformation of type (55), 10 signs change, while in the case of a transformation of type (56), 12 signs change. A sign change implies a restructuring of the intranuclear topology (i.e., a change in the convex-concave state of the local vacuum region inside and, possibly, outside the nucleus of the neutron), which requires energy expenditure. Therefore, the probability of a transformation with a change of 10 signs of type (55) is less energy-consuming and therefore more probable than a transformation of type (56) with a change of 12 signs.

This apparent asymmetry can be compensated for by considering the transformation of all six possible states of the neutron (53). Furthermore, the lower probability does not exclude the possibility of a decay of type (56). Therefore, the prediction of the possibility of a "neutron" decaying not only into a "proton" and "electron," but also into an "anti-proton" and "positron" must be thoroughly studied and experimentally verified.

Picoscopic topological (nodal) metamorphoses, during the transition of a "neutron" from one state (53) to another, occur so rapidly that for a macroscopic observer, a "neutron" is the result of averaging all six of its possible states.

$$n^0 = 1/6\,(n_1^0 + n_2^0 + n_3^0 + n_4^0 + n_5^0 + n_6^0) = 1/6\,(i_{\text{б}}^- d_{\text{г}}^+ d_{\text{з}}^+ u_{\text{к}}^- + i_{\text{б}}^- d_{\text{к}}^+ d_{\text{з}}^+ u_{\text{г}}^- + i_{\text{б}}^- d_{\text{к}}^+ d_{\text{г}}^+ u_{\text{з}}^- + i_{\text{б}}^+ d_{\text{г}}^- d_{\text{з}}^- u_{\text{к}}^+, + i_{\text{б}}^+ d_{\text{з}}^- d_{\text{к}}^- u_{\text{г}}^+, + i_{\text{б}}^+ d_{\text{г}}^- d_{\text{к}}^- u_{\text{з}}^+). \qquad (58)$$

The metric-dynamic model of the "neutron" proposed here provides an opportunity for a comprehensive study of this vacuum formation, which should be the subject of a separate, extensive study.

6. GVPh&AS is a modernized theory of general relativity

Before beginning the article devoted to the stochastic metric-dynamic model of the "hydrogen atom," let us recall the main aspects and provisions of the "Geometrized Vacuum Physics Based on the Algebra of Signature" (GVPh&AS) [1,2,3,4,5,6,7,8,9,10,11,12,13], which is essentially Einstein's modernized theory of general relativity (MoGR).

GVPh&AS relates to the vacuum as follows.

a) Within the framework of GVPh&AS, the vacuum (emptiness) is a 3-dimensional fluctuating boundary between two oceans: an infinite ocean of positive energy and an infinite ocean of negative energy. In each local volume of such a 3-dimensional boundary (i.e., vacuum), negative and positive energies do not completely compensate for each other's manifestations, therefore the vacuum is chaotically curved (fluctuates) everywhere, but when averaged over a sufficiently large area and/or over a sufficiently long period of time, all of its characteristics are equal to zero.

Let's explain this with an example: an infinite number of electromagnetic waves (EMWs) (from stars, galaxies, warm bodies, radio stations, power lines, cosmic microwave background radiation, etc.) arrive at each local region of a vacuum with a volume of, say, 1 mm³ (a conventional point in space). We know that if the EMW sources are incoherent, their intensities (energies) add up. Therefore, at each point in a vacuum, there should be an infinite amount of electromagnetic energy. But we don't sense this for two reasons. First, for every wave arriving at a given point, there is a virtually identical anti-wave with virtually the same frequency and amplitude, but coming from the opposite direction and/or with the opposite phase. Therefore, EMWs almost completely cancel each other out. Second, we are only able to distinguish and use energy gradients (differences), such as differences in temperature, pressure, intensity, density, potential, etc. That is, if one point in a vacuum contains an infinite amount of energy and a second nearby point contains approximately the same amount, we don't sense it and don't know how to use it. Therefore, on average, an uncurved region of vacuum is considered a low-potential void, although in fact it is extremely energetically saturated. We have considered only the electromagnetic component of vacuum energy; at each point in the vacuum, there are, on average, zero-point quark-gluon and Goldstone fluctuations, as well as gravitational fields from trillions of bodies, stars, planets, and so on. Thus, the vacuum is an extremely energetically saturated and complex three-dimensional space with, on average, zero-point characteristics.

b) In the GVPh&AS, a vacuum (i.e., an on-average zero-point 3-dimensional boundary between two mutually opposite oceans of positive and negative energies) is considered a continuous elastic-plastic medium, which potentially simultaneously possesses the properties of a liquid, a gas, a solid, and a plasma.

c) However, a vacuum is illusory for several reasons. First, a vacuum is absent under complete averaging. In §4 of [3], it was shown that a vacuum has at least two sides that are completely mutually opposite. At the next level of consideration (see §5.3 of [3]), a vacuum has 16 sides, but even in this case, they everywhere exclude each other's manifestations. At an even deeper level, a vacuum has 256 sides (intersecting layers), but even these are reduced to zero (see [1, 2, 3]). This transverse layering of the vacuum can continue indefinitely, but the complete superposition of the layers always leads to zero. Secondly, no matter how curved the extent of any layer of the vacuum, the Riemann geometry we use always allows the introduction of a local reference frame in which the components of the metric tensor correspond to uncurved Minkowski space. This means that there is nothing in this place.

When we sleep or daydream about something we've read or watched a movie, our consciousness perceives itself as occupying an illusory space filled with objects and events. A physical vacuum is fundamentally no different from such illusory spaces, except that the reality surrounding us is the same dream, continuing each time we awaken. When we attribute physical properties to a vacuum, we create another mental illusion, which can be called a dream within a dream. Of course, treating a vacuum as an illusion is not constructive (i.e., it's not suitable for increasing our technical and technological capabilities, or more precisely, for tailoring the illusion to our needs). But without such an attitude toward reality, we will never get closer to the Truth and will not understand how it is possible for the world to exist, but in reality, it doesn't.

d) Let us continue to treat vacuum as a ubiquitous real elastoplastic medium. In this case, within the framework of the GVPh&AS, it is proposed to introduce four main modifications into Einstein's general relativity:

1] Consider stable curvatures of the vacuum as solutions to the second and third Einstein vacuum equations with an infinite number of $\pm\Lambda_i$-terms

$$R_{ik} + ½ g_{ik}(\sum_{m=1}^{\infty}\Lambda_m + \sum_{n=1}^{\infty} - \Lambda_n) = 0, \tag{59}$$

which plays the role of 10 conservation laws (there are a total of 16 components of the Ricci tensor R_{ik}, but in Riemann geometry the symmetry $R_{ik} = R_{ki}$ takes place, so there are only 10 equations left, and, therefore, 10 conservation laws).

2] All theories and textbooks based on Einstein's general relativity use 4-dimensional metric spaces with one and/or two signatures $(+---)$ and/or $(-+++)$. However, the GVPh&AS takes into account the intersection of all 16 possible types of 4-dimensional metric spaces with the following signatures (i.e., topologies, see §4 in [2])

$$sign\left(ds^{(a,b)2}\right) = \begin{pmatrix} (++++) & (+++-) & (-++-) & (++-+) \\ (---+) & (-+++) & (--++) & (-+-+) \\ (+--+) & (++--) & (+---) & (+-++) \\ (--+-) & (+-+-) & (-+--) & (----) \end{pmatrix}. \tag{60}$$

3] Just as in GTR, the solution to Einstein's vacuum equations are metrics of the form

$$\begin{aligned} s_0^2 = \; & g_{00}c^2dtdt - g_{10}dxcdt - g_{20}dycdt - g_{30}dzcdt - \\ & -g_{01}\mathrm{c}dtdx - g_{11}dxdx + g_{21}dydx + g_{31}dzdx - \\ & -g_{02}\mathrm{c}dtdy + g_{12}dxdy - g_{22}dydy + g_{32}dzdy - \\ & -g_{03}\mathrm{c}dtdz + g_{13}dxdz + g_{23}dydz - g_{33}dzdz. \end{aligned} \tag{61}$$

But the components of the metric tensor g_{ij} have a fundamentally different interpretation. In the framework of the GVPh&AS *cdt, dx, dy, dz* are infinitely small segments on four fictitious axes *ct, x, y, z* (where *t* is Newtonian time, which flows everywhere equally, linearly and uniformly; *x, y, z* are the coordinates of a point in three-dimensional space, auxiliary for our perception of the surrounding extended existence);

g_{00} (t, x, y, z) is the zero component of the metric tensor, which determines the laminar (rectilinear) component of the vacuum layer flow at a point with coordinates *t, x, y, z* (see §6.2 in [3] and §4 in [4]);

$g_{0\alpha}$ $(t, x, y, z) = g_{\alpha 0}$ (t, x, y, z) (where α = 1,2,3) determine the rotational components of the vacuum layer motion at the point with coordinates *t, x, y, z* (see §6.2 in [3] and §4 in [4]);

$g_{\alpha\beta}$ $(t, x, y, z) = g_{\beta\alpha}$ (t, x, y, z) (where $\alpha, \beta = 1,2,3$) is determine the deformations of a local section of the vacuum layer at the point with coordinates *t,x,y,z* (see §6.1 in [3]).

The velocity of a local region of one of the vacuum layers is determined by comparing g_{00} and $g_{0\alpha}$ with the analogous components of the metric tensor from the corresponding kinematic metric (see §6.2 in [3] and §2.2 in [7]).

In the stationary case, when $g_{ij}(x, y, z) = const$ (i.e., independent of time *t*), the acceleration of a local region of one of the vacuum layers is determined by substituting g_{ij} into Eq. (108) in [4] (see §§4 and 5 in [4]).

The deformations of a local region of one of the vacuum layers in the GVPh&AS are judged by the components of the metric tensor $g_{\alpha\beta}$, when they are substituted into the equations for determining the relative elongation vector; see §5.1 in [3].

Taking into account the velocities, accelerations and deformations of all 2 (or 16, or 256, etc.) vacuum layers simultaneously is considered in [4].

4] Another significant difference between the GVPh&AS and Einstein's General Relativity is that the proposed theory does not contain any massive bodies that create a curvature of space-time around themselves, and there is no physical quantity of mass with the dimension of a kilogram. In the GVPh&AS, there are only various distortions, curvatures, and displacements of entangled layers of vacuum (see Figure 3*a*). Moreover, among the many different entangled distortions of the vacuum extent, there are stable convex or concave states of vacuum (Figure 3b), consisting of "quarks" and "antiquarks" of various colors and sizes (see Table 1 in [6], Table 1 in [10], Table 1 in [12]), which individually or collectively satisfy the conservation laws (i.e., Einstein's second vacuum equation, see §3 in [5]). Within the framework of the GVPh&AS, such stable convex or concave vacuum formations are respectively called “corpuscles” or “anticorpuscles” of picoscopic, microscopic, planetary, galactic, and other scales.

a)

b)

Fig. 3: a) Fractal illustration of intertwined vacuum layers within the framework of the GVPh&AS concepts; b) Fractal illustration of the core of a "corpuscle" (on average, a convex vacuum formation)

Based on the above modifications of General Relativity, a 10-level Hierarchical Cosmological Model was proposed in a series of articles under the general title [5,6,7,8,10,11,12]. This model posits that a closed mega-Universe is filled with an infinite number of "corpuscles" (i.e., "particles") of 10 main types (see Figure 4a) with a discrete set of characteristic (approximate) radii of their cores (44a) in [6]:

$r_1 \sim 10^{39}$ cm is radius of the mega-Universe; (62)
$r_2 \sim 10^{28}$ cm is radius of the observable Universe;
$r_3 \sim 10^{17}$ cm is radius of the galactic core;
$r_4 \sim 10^{7}$ cm is radius of the core of a planet or star;
$r_5 \sim 10^{-3}$ cm is radius of a biological cell;
$r_6 \sim 10^{-13}$ cm is radius of an elementary particle core;
$r_7 \sim 10^{-24}$ cm is radius of a proto-quark core;
$r_8 \sim 10^{-34}$ cm is radius of a plankton core;
$r_9 \sim 10^{-45}$ cm is radius of the proto-plankton core;
$r_{10} \sim 10^{-55}$ cm is radius of the instanton core.

These "corpuscles" are nested like Russian dolls (see Figure 4b).

The hierarchy of radii rm (62) was obtained using the heuristic (estimative) recurrence formula (43) in [6]:

$$r_m \sim \frac{R_v^2}{l_v^m} = \frac{R_v^2}{(3\cdot 10^{10})^m} \text{ cm}, \tag{63}$$

where $R_v \approx 10^{25}$ cm is the parametric radius of the Universe. (64)

5] The fifth significant difference between the GVPh&AS and GTR is that in GTR, celestial bodies move smoothly along deterministic geodesic lines of curved space, whereas in the GVPh&AS, these deterministic (smooth) trajectories are only the mean lines of motion of the cores of vacuum formations. Moreover, the cores of all picoscopic, microscopic, planetary, galactic, and other "corpuscles" with orientation radii (62) are like clots of quivering jelly, which are constantly bizarrely distorted (Figures 3b and 4b) and constantly chaotically deviate from the mean line of their motion due to the fact that the vacuum is chaotically fluctuating (distorted) everywhere. In other words, in the GVPh&AS, Einstein's vacuum equations determine only the average spherical shapes of the cores of the "corpuscles" and the average trajectories of their motion.

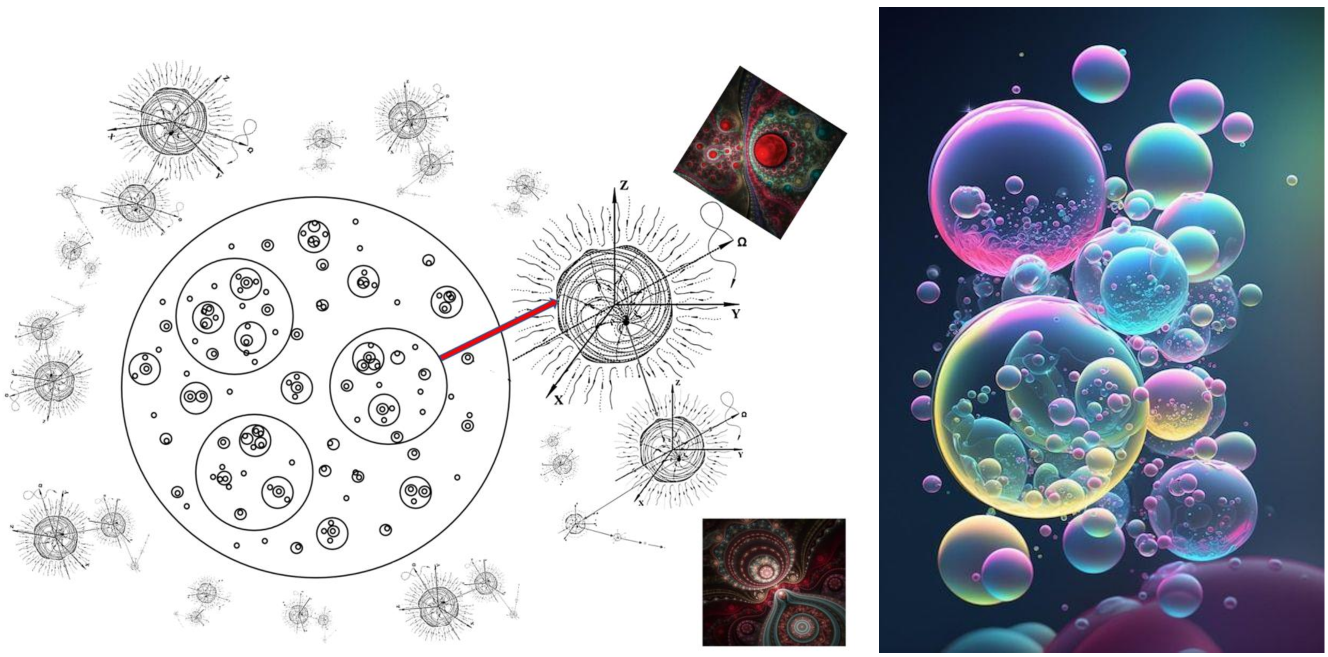

a) *b*)

Fig. 4: a) Schematic representation of the Hierarchical Cosmological Model, consisting of an infinite number of hierarchical chains of “corpuscles” and “anticorpuscles” of various sizes (62), nested inside each other like Russian dolls; b) One of the infinite number of hierarchical chains, consisting of “corpuscles” nested inside each other; c) Illustration of the multi-level organization of stable vacuum formations, nested inside each other like Russian dolls

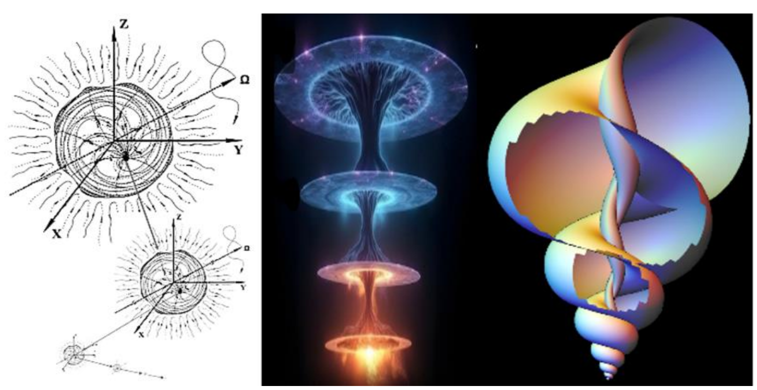

c)

To describe the chaotic behavior of nuclei of all types of "corpuscles," they are considered stochastic systems whose average behavior is predetermined by two fundamental, relentlessly entraining tendencies: the principle of "minimum action" and the principle of "maximum entropy." The simultaneous stochastic system's tendency toward Order (i.e., toward energy and information conservation) and Chaos (i.e., toward the ultimate redistribution of possible states) is determined by the form factors and energy resources of these systems. In [13,14], the dichotomy (i.e., the bifurcation of the unified) into Order and Chaos is expressed as the principle of "extremum efficiency." The equations for finding extremals of the "efficiency of a stochastic system" functional turned out to be differential equations of diffusion theory, Brownian motion, and, in particular, the Schrödinger equation (see [13,14]).

Thus, within the framework of the GVPh&AS, there are no contradictions between Einstein's modernized general relativity (MGR) and Edward Nelson's stochastic quantum mechanics (SQM). These theories complement each other: MGR describes "corpuscles" as averaged stable deformations of the vacuum and their average trajectories, while SQM describes the chaotic behavior of their nuclei, associated with the fact that the vacuum everywhere chaotically fluctuates and trembles.

6]. Einstein's general relativity theory underlies modern cosmological models. After the James Webb Space Telescope discovered formed galaxies at a distance of approximately 13.5 billion light-years, the validity of the Big Bang theory and, with it, the validity of the ΛCDM-standard cosmological model came into serious question. Consequently, various scenarios for changing scientific understanding of the development of the Universe began to emerge, inevitably entailing a modernization of general relativity.

The vacuum physics proposed here is inherently inconsistent with the Big Bang theory and is based on the modernizations of general relativity outlined above. At the same time, the GVPh&AS and the Hierarchical Cosmological Model are based on esoteric cosmic mythology. According to ancient views, our Universe is the Mother's Womb in which the Cosmic Embryo (Eternal Man) developed (see Figure 5a). The stages of expansion of the Mother's Womb and the growth of the Embryo within Her largely coincide with the stages of the Universe's development within the Big Bang theory. At a certain early stage, the Universal Man acquired freedom of choice and allowed the outer darkness within himself (ate the forbidden fruit), resulting in a colossal tragedy known as the "shattering of the Vessels." The Universe became covered with a network of three-dimensional cracks of varying sizes (see Figure 5b), many of which closed into hard shells (the nuclei of "corpuscles") of varying sizes (see Figures 4 and 5c).

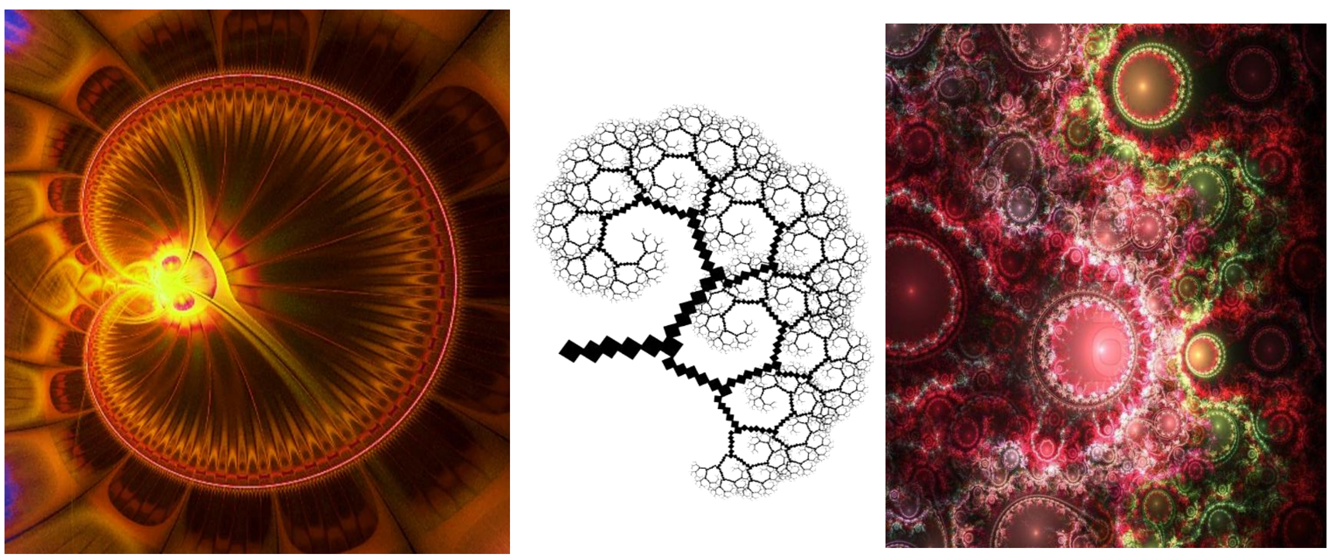

a) b) c)

Fig. 5: Stages of the esoteric gestational cosmological model

After the "shattering of the vessels," the Universe plunged into chaos, in which the vacuum boiled and the nuclei of "corpuscles" of all sizes and types seethed, but in a percentage ratio dependent on the simplicity of the "corpuscle." The simpler the "corpuscles," the more numerous they were. Thus, with the grandiose "shattering of the vessels," shells of all sizes (i.e., core of "atoms" and most "molecules" of all scales) arose simultaneously: ioctoscopic ($\sim 10^{-24}$ cm), picoscopic ($\sim 10^{-13}$ cm), microscopic ($\sim 10^{-3}$ cm), stellar-planetary ($\sim 10^{-7}$cm), galactic ($\sim 10^{-17}$ cm), etc., nested one inside another like Russian dolls (see Figure 4). After a period of intense chaos, as the Mother's Womb expanded, the "broth" cooled, and the cores of large "corpuscles" (for example, the cores of "galaxies," as well as the cores of "planets" and "stars") began to gather around themselves the nuclei (shells) of smaller "corpuscles," leading to the cleansing of the cosmos from "fragments" and the further Evolution of Consciousness. This gestational cosmological scenario could explain why galaxies formed significantly earlier than predicted by the ΛCDM-cosmological model.

MATERIALS AND METHODS

This article (Part 14 of the GVPh&AS) considers only the stochastic metric-dynamic model (MDM) of the "hydrogen atom." However, the mathematical apparatus and methods for studying this stable vacuum structure (topological knot) are suitable for constructing similar models and studying all "atoms" from D.I. Mendeleev's periodic table of chemical elements.

1. Stochastic metric-dynamic model of the "hydrogen atom"

First, let us consider the "hydrogen atom" as, on average, a stable spherical vacuum structure in a quiescent state. Stationary "atoms" do not exist in reality; they are all constantly in chaotic (thermal) motion. The metric-dynamic model (MDM) of a moving vacuum structure becomes significantly more complex (see [8]). Therefore, to identify the basic framework (a kind of skeleton) of the "hydrogen atom," we conventionally assume that it is stationary.

As is known from nuclear physics, a hydrogen atom consists of one proton and one electron. Within the framework of the GVPh&AS, a neutral "hydrogen atom" consists of "quarks" and "antiquarks" from Table 1. A "hydrogen atom" can have the following six possible nodal (signature, or topological) configurations:

$$\begin{array}{l} e_{\text{ж}}^{+}(+\ -\ -\ -) \\ d_{\text{к}}^{+}(+\ +\ +\ -) \\ u_{\text{з}}^{-}(-\ +\ -\ +) \\ u_{\text{г}}^{-}\underline{(-\ -\ +\ +)} \\ H_1^{+}(0\ 0\ 0\ 0)_{+} \end{array} \quad (65) \qquad \begin{array}{l} e_{\text{ж}}^{+}(+\ -\ -\ -) \\ d_{\text{з}}^{+}(+\ +\ -\ +) \\ u_{\text{г}}^{-}(-\ -\ +\ +) \\ u_{\text{к}}^{-}\underline{(-\ +\ +\ -)} \\ H_2^{+}(0\ 0\ 0\ 0)_{+} \end{array} \quad (66) \qquad \begin{array}{l} e_{\text{ж}}^{+}(+\ -\ -\ -) \\ d_{\text{г}}^{+}(+\ -\ +\ +) \\ u_{\text{к}}^{-}(-\ +\ +\ -) \\ u_{\text{з}}^{-}\underline{(-\ +\ -\ +)} \\ H_3^{+}(0\ 0\ 0\ 0)_{+} \end{array} \quad (67)$$

$$\begin{array}{l} e_{\text{ж}}^{-}(-\ +\ +\ +) \\ d_{\text{к}}^{-}(-\ -\ -\ +) \\ u_{\text{з}}^{+}(+\ -\ +\ -) \\ u_{\text{г}}^{+}\underline{(+\ +\ -\ -)} \\ H_4^{-}(0\ 0\ 0\ 0)_{+} \end{array} \quad (68) \qquad \begin{array}{l} e_{\text{ж}}^{-}(-\ +\ +\ +) \\ d_{\text{з}}^{-}(-\ -\ +\ -) \\ u_{\text{г}}^{+}(+\ +\ -\ -) \\ u_{\text{к}}^{+}\underline{(+\ -\ -\ +)} \\ H_5^{-}(0\ 0\ 0\ 0)_{+} \end{array} \quad (69) \qquad \begin{array}{l} e_{\text{ж}}^{-}(-\ +\ +\ +) \\ d_{\text{г}}^{-}(-\ +\ -\ -) \\ u_{\text{к}}^{+}(+\ -\ -\ +) \\ u_{\text{з}}^{+}\underline{(+\ -\ +\ -)} \\ H_6^{-}(0\ 0\ 0\ 0)_{+} \end{array} \quad (70)$$

The first three nodal (topological) configurations of the "hydrogen atom" (65) – (67) consist of one "electron" (i.e., the yellow e_y^{+}-"quark" from Table 1) (11) and three colored p_i^{-}-"proton" configurations (31) – (33), where each signature in the numerator of these rankings corresponds to a set of 10 metrics of the form (40) – (48).

The second three nodal (topological) configurations of the "hydrogen atom" (68) – (70) consist of one "positron" (i.e., one yellow e_y^{+}-"antiquark" from Table 1) (21) and three colored p_i^{+}-"antiproton" configurations (34)– (36).

Despite the fact that the nodal configurations (65) – (67) and (69) – (70) are completely opposite to each other, within the framework of the GVPh&AS, they are all, on average, neutral (i.e., have a zero signature (0 0 0 0), are practically indistinguishable, and do not annihilate (due to the fact that for annihilation, they must be absolutely exact anti-copies of each other, and this is practically impossible due to their constant internal metamorphosis and external thermal motion).

Apparently, we have not an "atom" and an "anti-atom," but two types of "hydrogen atom":

- a positive (female) "hydrogen atom," taking into account (50),

$$H^{+} = 1/3\ (H_1^{+} + H_2^{+} + H_3^{+}) = 1/3(e_y^{+}\, u_g^{-}\, u_b^{-}\, d_r^{+}\ +\ e_y^{+}\, u_r^{-}\, u_b^{-}\, d_g^{+}\ +\ e_y^{+}\, u_g^{-}\, u_r^{-}\, d_b^{+}) \quad (71)$$

- negative (male) "hydrogen atom," taking into account (52);

$$H^{-} = 1/3\ (H_1^{-} + H_2^{-} + H_3^{-}) = 1/3(e_y^{-}\, u_g^{+}\, u_b^{+}\, d_r^{-}\ +\ e_y^{-}\, u_r^{+}\, u_b^{+}\, d_g^{-}\ +\ e_y^{-}\, u_g^{+}\, u_r^{+}\, d_b^{-}).$$

This statement requires experimental verification, but distinguishing between them will not be easy, since, as will be shown below, the "atoms" H^{+} and H^{-} have identical absorption and emission spectra.

For example, let's imagine a metric-dynamic model of a "hydrogen atom" at rest in configuration (67)

$$\begin{array}{l} e_{ж}^{+}(+\ -\ -\ -) \\ d_{г}^{+}(+\ -\ +\ +) \\ u_{к}^{-}(-\ +\ +\ -) \\ \underline{u_{з}^{-}(-\ +\ -\ +)} \\ H_3^{+}(0\ \ 0\ \ 0\ \ 0)_{+} \end{array} \qquad (67')$$

in expanded form

H_1^{+}-"HYDROGEN ATOM" (72)

a stable, on average, neutral spherical vacuum formation at rest
with the general signature (0 0 0 0), consisting of one "electron" (or e_y^{+}-"quark"),
d_b^{+}-"quark", u_r^{-}-"antiquark", and u_g^{-}-"antiquark":

e_y^{+}-"quark"

(or "ELECTRON") (73)

is, on average, a spherical, stable, convex, multilayered
vacuum curvature with a signature (+ – – –), consisting of:

The outer shell of the "electron"

in the interval [r_1,r_6] (Figure 1a), with a signature (+ – – –) (74)

I $$ds_{1,1}^{(+---)2} = \left(1 - \frac{r_{6,1,1}}{r} + \frac{r^2}{r_L^2}\right) c^2dt^2 - \frac{dr^2}{\left(1 - \frac{r_{6,1,1}}{r} + \frac{r^2}{r_L^2}\right)} - r^2(d\theta^2 + sin^2\,\theta\, d\phi^2), \qquad (75)$$

H $$ds_{2,1}^{(+---)2} = \left(1 + \frac{r_{6,1,2}}{r} - \frac{r^2}{r_L^2}\right) c^2dt^2 - \frac{dr^2}{\left(1 + \frac{r_{6,1,2}}{r} - \frac{r^2}{r_L^2}\right)} - r^2(d\theta^2 + sin^2\,\theta\, d\phi^2), \qquad (76)$$

V $$ds_{3,1}^{(+---)2} = \left(1 - \frac{r_{6,1,3}}{r} - \frac{r^2}{r_L^2}\right) c^2dt^2 - \frac{dr^2}{\left(1 - \frac{r_{6,1,3}}{r} - \frac{r^2}{r_L^2}\right)} - r^2(d\theta^2 + sin^2\,\theta\, d\phi^2), \qquad (77)$$

H′ $$ds_{4,1}^{(+---)2} = \left(1 + \frac{r_{6,1,4}}{r} + \frac{r^2}{r_L^2}\right) c^2dt^2 - \frac{dr^2}{\left(1 + \frac{r_{6,1,4}}{r} + \frac{r^2}{r_L^2}\right)} - r^2(d\theta^2 + sin^2\,\theta\, d\phi^2); \qquad (78)$$

The "electron's" core (79)

in the interval [r_6, r_9] (Figure 1a), with the signature (+ – – –)

I $$ds_{1,2}^{(+---)2} = \left(1 + \frac{r_S}{r} - \frac{r^2}{r_{6,2,1}^2}\right) c^2dt^2 - \frac{dr^2}{\left(1 + \frac{r_S}{r} - \frac{r^2}{r_{6,2,1}^2}\right)} - r^2(d\theta^2 + sin^2\,\theta\, d\phi^2), \qquad (80)$$

H $$ds_{2,2}^{(,+---)2} = \left(1 - \frac{r_S}{r} + \frac{r^2}{r_{6,2,2}^2}\right) c^2dt^2 - \frac{dr^2}{\left(1 - \frac{r_S}{r} + \frac{r^2}{r_{6,2,2}^2}\right)} - r^2(d\theta^2 + sin^2\,\theta\, d\phi^2), \qquad (81)$$

V $$ds_{3,2}^{(+---)2} = \left(1 + \frac{r_S}{r} + \frac{r^2}{r_{6,2,3}^2}\right) c^2dt^2 - \frac{dr^2}{\left(1 + \frac{r_S}{r} - \frac{r^2}{r_{6,2,3}^2}\right)} - r^2(d\theta^2 + sin^2\,\theta\, d\phi^2), \qquad (82)$$

H′ $$ds_{4,2}^{(+---)2} = \left(1 - \frac{r_S}{r} - \frac{r^2}{r_{6,2,4}^2}\right) c^2dt^2 - \frac{dr^2}{\left(1 - \frac{r_S}{r} - \frac{r^2}{r_{6,2,4}^2}\right)} - r^2(d\theta^2 + sin^2\,\theta\, d\phi^2); \qquad (83)$$

The substrate of the "electron"

in the interval [0, ∞], signature (+ – – –)

i $$ds_{5.1}^{(+---)2} = c^2dt^2 - dr^2 - r^2(d\theta^2 + sin^2\,\theta\, d\phi^2). \qquad (84)$$

d_b^{+}-"quark" (85)

a convex-concave vacuum formation
with the signature (+ – + +), consisting of:

The outer shell of the d_b^{+}-"quark" (86)

in the interval [r_5,r_6] (Figure 2), signature (+ – + +)

I $$ds_{1,3}^{(+++-)2} = \left(1 - \frac{r_{6,3,1}}{r} + \frac{r^2}{r_L^2}\right) c^2dt^2 - \frac{dr^2}{\left(1 - \frac{r_{6,3,1}}{r} + \frac{r^2}{r_L^2}\right)} + r^2d\theta^2 + r^2\,sin^2\,\theta\, d\phi^2, \qquad (87)$$

H $$ds_{2,3}^{(+++-)2} = \left(1 + \frac{r_{6,3,2}}{r} - \frac{r^2}{r_L^2}\right) c^2dt^2 - \frac{dr^2}{\left(1+\frac{r_{6,3,2}}{r} - \frac{r^2}{r_L^2}\right)} + r^2d\theta^2 + r^2 \sin^2\theta\, d\phi^2, \quad (88)$$

V $$ds_{3,3}^{(+++-)2} = \left(1 - \frac{r_{6,3,3}}{r} - \frac{r^2}{r_L^2}\right) c^2dt^2 - \frac{dr^2}{\left(1-\frac{r_{6,3,3}}{r} - \frac{r^2}{r_L^2}\right)} + r^2d\theta^2 + r^2 \sin^2\theta\, d\phi^2, \quad (89)$$

H′ $$ds_{4,3}^{(+++-)2} = \left(1 + \frac{r_{6,3,4}}{r} + \frac{r^2}{r_L^2}\right) c^2dt^2 - \frac{dr^2}{\left(1+\frac{r_{6,3,4}}{r} + \frac{r^2}{r_L^2}\right)} + r^2d\theta^2 + r^2 \sin^2\theta\, d\phi^2; \quad (90)$$

The d_b^+-"quark's" core (91)

in the interval [r_6,r_9] (Figure 2), with the signature (+ – + +)

I $$ds_{1,4}^{(+-++)2} = \left(1 - \frac{r_S}{r} + \frac{r^2}{r_{6,4,1}^2}\right) c^2dt^2 - \frac{dr^2}{\left(1-\frac{r_S}{r} + \frac{r^2}{r_{6,4,1}^2}\right)} + r^2d\theta^2 + r^2 \sin^2\theta\, d\phi^2, \quad (92)$$

H $$ds_{2,4}^{(+-++)2} = \left(1 + \frac{r_S}{r} - \frac{r^2}{r_{6,4,2}^2}\right) c^2dt^2 - \frac{dr^2}{\left(1+\frac{r_S}{r} - \frac{r^2}{r_{6,4,2}^2}\right)} + r^2d\theta^2 + r^2 \sin^2\theta\, d\phi^2, \quad (93)$$

V $$ds_{3,4}^{(+-++)2} = \left(1 - \frac{r_S}{r} - \frac{r^2}{r_{6,4,4}^2}\right) c^2dt^2 - \frac{dr^2}{\left(1-\frac{r_S}{r} - \frac{r^2}{r_{6,4,3}^2}\right)} + r^2d\theta^2 + r^2 \sin^2\theta\, d\phi^2, \quad (94)$$

H′ $$ds_{4,4}^{(+-++)2} = \left(1 + \frac{r_S}{r} + \frac{r^2}{r_{6,4,5}^2}\right) c^2dt^2 - \frac{dr^2}{\left(1+\frac{r_S}{r} + \frac{r^2}{r_{6,4,4}^2}\right)} + r^2d\theta^2 + r^2 \sin^2\theta\, d\phi^2; \quad (95)$$

The substrate of the d_b^+-"quark" (96)

in the interval [0, ∞], signature (+ – + +)

i $$s_{5,2}^{(+-++)2} = c^2dt^2 + dr^2 - r^2d\theta^2 + r^2 \sin^2\theta\, d\phi^2. \quad (97)$$

u_r^-- "antiquark" (98)

a concave-convex vacuum formation with a signature (– + + –), consisting of:

The outer shell of the u_r^--"antiquark" (99)

in the interval [r_5,r_6] (Figure 2), signature (– + + –)

I $$ds_{1,5}^{(-++-)2} = -\left(1 - \frac{r_{6,5,1}}{r} + \frac{r^2}{r_L^2}\right) c^2dt^2 + \frac{dr^2}{\left(1-\frac{r_{6,5,1}}{r} + \frac{r^2}{r_L^2}\right)} + r^2d\theta^2 - r^2 \sin^2\theta\, d\phi^2, \quad (100)$$

H $$ds_{2,5}^{(-++-)2} = -\left(1 + \frac{r_{6,5,2}}{r} - \frac{r^2}{r_L^2}\right) c^2dt^2 + \frac{dr^2}{\left(1+\frac{r_{6,5,2}}{r} - \frac{r^2}{r_L^2}\right)} + r^2d\theta^2 - r^2 \sin^2\theta\, d\phi^2, \quad (101)$$

V $$ds_{3,5}^{(-++-)2} = -\left(1 - \frac{r_{6,5,3}}{r} - \frac{r^2}{r_L^2}\right) c^2dt^2 + \frac{dr^2}{\left(1-\frac{r_{6,5,3}}{r} - \frac{r^2}{r_L^2}\right)} + r^2d\theta^2 - r^2 \sin^2\theta\, d\phi^2, \quad (102)$$

H′ $$ds_{4,5}^{(-++-)2} = -\left(1 + \frac{r_{6,5,4}}{r} + \frac{r^2}{r_L^2}\right) c^2dt^2 + \frac{dr^2}{\left(1+\frac{r_{6,5,4}}{r} + \frac{r^2}{r_L^2}\right)} + r^2d\theta^2 - r^2 \sin^2\theta\, d\phi^2; \quad (103)$$

The u_r^--"antiquark's" core (104)

in the interval [r_6,r_9] (Figure 2), with the signature (– + + –)

I $$ds_{1,6}^{(-++-)2} = -\left(1 - \frac{r_S}{r} + \frac{r^2}{r_{6,6,1}^2}\right) c^2dt^2 + \frac{dr^2}{\left(1-\frac{r_S}{r} + \frac{r^2}{r_{6,6,1}^2}\right)} + r^2d\theta^2 - r^2 \sin^2\theta\, d\phi^2, \quad (105)$$

H $$ds_{2,6}^{(-++-)2} = -\left(1 + \frac{r_S}{r} - \frac{r^2}{r_{6,6,2}^2}\right) c^2dt^2 + \frac{dr^2}{\left(1+\frac{r_S}{r} - \frac{r^2}{r_{6,6,2}^2}\right)} + r^2d\theta^2 - r^2 \sin^2\theta\, d\phi^2, \quad (106)$$

V $$ds_{3,6}^{(-++-)2} = -\left(1 - \frac{r_S}{r} - \frac{r^2}{r_{6,6,3}^2}\right) c^2dt^2 + \frac{dr^2}{\left(1-\frac{r_S}{r} - \frac{r^2}{r_{6,6,3}^2}\right)} + r^2d\theta^2 - r^2 \sin^2\theta\, d\phi^2, \quad (107)$$

H′ $$ds_{4,6}^{(-++-)2} = -\left(1 + \frac{r_S}{r} + \frac{r^2}{r_{6,6,4}^2}\right) c^2dt^2 + \frac{dr^2}{\left(1+\frac{r_S}{r} + \frac{r^2}{r_{6,6,4}^2}\right)} + r^2d\theta^2 - r^2 \sin^2\theta\, d\phi^2; \quad (108)$$

The substrate of the u_r^--"antiquark" (109)

in the interval [0, ∞], signature (– + + –)

i $$ds_{5,3}^{(-++-)2} = -c^2dt^2 + dr^2 + r^2d\theta^2 - r^2 \sin^2\theta\, d\phi^2. \quad (110)$$

u_g^-- "antiquark" (111)

a concave-convex vacuum formation with a signature (– + – +), consisting of:

The outer shell of the u_g^--"antiquark" (112)

in the interval [r_5,r_6] (Figure 2), signature (– + – +)

I $$ds_{1,7}^{(-+-+)2} = -\left(1 - \frac{r_{6,7,1}}{r} + \frac{r^2}{r_L^2}\right)c^2dt^2 + \frac{dr^2}{\left(1 - \frac{r_{6,7,1}}{r} + \frac{r^2}{r_L^2}\right)} - r^2d\theta^2 + r^2 \sin^2\theta\, d\phi^2, \quad (113)$$

H $$ds_{2,7}^{(-+-+)2} = -\left(1 + \frac{r_{6,7,2}}{r} - \frac{r^2}{r_L^2}\right)c^2dt^2 + \frac{dr^2}{\left(1 + \frac{r_{6,7,2}}{r} - \frac{r^2}{r_L^2}\right)} - r^2d\theta^2 + r^2 \sin^2\theta\, d\phi^2, \quad (114)$$

V $$ds_{3,7}^{(-+-+)2} = -\left(1 - \frac{r_{6,7,3}}{r} - \frac{r^2}{r_L^2}\right)c^2dt^2 + \frac{dr^2}{\left(1 - \frac{r_{6,7,3}}{r} - \frac{r^2}{r_L^2}\right)} - r^2d\theta^2 + r^2 \sin^2\theta\, d\phi^2, \quad (115)$$

H′ $$ds_{4,7}^{(-+-+)2} = -\left(1 + \frac{r_{6,7,4}}{r} + \frac{r^2}{r_L^2}\right)c^2dt^2 + \frac{dr^2}{\left(1 + \frac{r_{6,7,4}}{r} + \frac{r^2}{L}\right)} - r^2d\theta^2 + r^2 \sin^2\theta\, d\phi^2; \quad (116)$$

The u_g^--"antiquark's" core (117)

in the interval [r_6,r_9] (Figure 2), with the signature (– + – +)

I $$ds_{1,8}^{(-+-+)2} = -\left(1 - \frac{r_S}{r} + \frac{r^2}{r_{6,8,1}^2}\right)c^2dt^2 + \frac{dr^2}{\left(1 - \frac{r_S}{r} + \frac{r^2}{r_{6,8,1}^2}\right)} - r^2d\theta^2 + r^2 \sin^2\theta\, d\phi^2, \quad (118)$$

H $$ds_{2,8}^{(-+-+)2} = -\left(1 + \frac{r_S}{r} - \frac{r^2}{r_{6,8,2}^2}\right)c^2dt^2 + \frac{dr^2}{\left(1 + \frac{r_S}{r} - \frac{r^2}{r_{6,8,2}^2}\right)} - r^2d\theta^2 + r^2 \sin^2\theta\, d\phi^2, \quad (119)$$

V $$ds_{3,8}^{(--++)2} = -\left(1 - \frac{r_S}{r} - \frac{r^2}{r_{6,8,3}^2}\right)c^2dt^2 + \frac{dr^2}{\left(1 - \frac{r_S}{r} - \frac{r^2}{r_{6,8,3}^2}\right)} - r^2d\theta^2 + r^2 \sin^2\theta\, d\phi^2, \quad (120)$$

H′ $$ds_{4,8}^{(-+-+)2} = -\left(1 + \frac{r_S}{r} + \frac{r^2}{r_{6,8,4}^2}\right)c^2dt^2 + \frac{dr^2}{\left(1 + \frac{r_S}{r} + \frac{r^2}{r_{6,8,4}^2}\right)} - r^2d\theta^2 + \sin^2\theta\, d\phi^2; \quad (121)$$

The substrate of the u_g^--"antiquark"

in the interval [0, ∞], signature (– + – +)

i $$ds_{5,4}^{(-+-+)2} = -c^2dt^2 + dr^2 - r^2d\theta^2 + r^2 \sin^2\theta\, d\phi^2. \quad (122)$$

2. The outer shell of the "hydrogen atom"

We will consider the metric-dynamic model of the outer shell of the "hydrogen atom" using the set of metrics (i.e., quadratic forms) (73) – (119) for the nodal (topological) confirmation (67). For nodal configurations (65), (66), (68), (69), and (70), we obtain similar results.

The outer shell of the "hydrogen atom" in configuration (67) is a superposition (or averaging) of the outer shells of "quarks" and "antiquarks" (75) – (78) + (87) – (91) + (101) – (104) + (113) – (116). Let us assume that the radii of the nuclei of all the "quarks" and "antiquarks" that make up the "hydrogen atom" are practically the same, i.e., the radii r_(6,i,j) in the metrics (75) – (78), (87) – (91), (101) – (104), (113) – (116) are approximately are equal to

$r_{6,1,1} \approx r_{6,1,2} \approx r_{6,1,3} \approx r_{6,1,4} \approx r_{6,3,1} \approx r_{6,3,2} \approx r_{6,3,3} \approx r_{6,3,4} \approx r_{6,5,1} \approx r_{6,5,2} \approx r_{6,5,3} \approx r_{6,5,4} \approx r_{6,7,1} \approx r_{6,7,2} \approx r_{6,7,3} \approx r_{6,7,4}$.

Then the addition (or averaging) of all metrics ((75) – (78), (87) – (91), (101) – (104), (113) – (116) according to rule (67) is approximately equal to zero. Indeed,

$$ds_{1,1}^{(+---)2} + ds_{1,3}^{(+++-)2} + ds_{1,5}^{(-++-)2} + ds_{1,7}^{(-+-+)2} \approx 0, \quad (123)$$

$$ds_{2,1}^{(+---)2} + ds_{2,3}^{(+++-)2} + ds_{2,5}^{(-++-)2} + ds_{2,7}^{(-+-+)2} \approx 0, \quad (124)$$

$$ds_{3,1}^{(+---)2} + ds_{3,3}^{(+++-)2} + ds_{3,5}^{(-++-)2} + ds_{3,7}^{(-+-+)2} \approx 0, \quad (125)$$

$$ds_{4,1}^{(+---)2} + ds_{3,3}^{(+++-)2} + ds_{4,5}^{(-++-)2} + ds_{4,7}^{(-+-+)2} \approx 0. \quad (126)$$

The total sum of metrics (123) – (126) is also approximately zero: 0 + 0 + 0 + 0 ≈ 0.

Within the framework of the GVPh&AS, this means that in the outer shell of a stationary "hydrogen atom," all vacuum layers, on average, compensate for each other's effects: deformations are compensated by anti-deformations, and flows (intra-vacuum currents) are compensated by anti-flows (opposite intra-vacuum currents). However, due to the incomplete compensation of these multilayer effects, chaotic vacuum fluctuations remain in the vicinity of the "hydrogen atom's" core (with dimensions on the order of the radius of the "proton's" core, see Figure 2), but these, too, are, on average, zero. In other words, at each point in the vicinity of the "hydrogen atom's" core, these fluctuations can be viewed as a random process with zero mathematical expectation:

Fractal illustration of vacuum deformations and intertwining of intra-vacuum currents in the vicinity of the core of a neutral "atom", revealed by the mathematical apparatus of "Geometrized Vacuum Physics Based on the Algebra of Signature " (GVPh&AS), which, on average, are zero.

The question arises: If, on average, deformations and flows are not observed in the outer shell of the "hydrogen atom," do they exist in principle or not? The answer to this question, to some extent, corresponds to the answer to the question: Do sine and cosine waves exist in the spectrum of analog signals? However, vacuum fluctuations, despite being zero on average, manifest themselves in processes that will be discussed below.

3. The core of the "hydrogen atom"

The core of the "hydrogen atom" in configuration (67) is the result of the summation (or averaging) of the cores of the "electron" (or e_y^+-"quark") (79), the d_b^+-"quark" (92), the u_r^--"antiquark" (105), and the u_g^--"antiquark" (117). Provided that the radii of these nuclei are approximately equal to r_6.

$$r_6 \approx r_{6,2,1} \approx r_{6,2,2} \approx r_{6,2,3} \approx r_{6,2,4} \approx r_{6,4,1} \approx r_{6,4,2} \approx r_{6,4,3} \approx r_{6,4,4} \approx r_{6,6,1} \approx r_{6,6,2} \approx r_{6,6,3} \approx r_{6,6,4} \approx r_{6,8,1} \approx r_{6,8,2} \approx r_{6,7,3} \approx r_{6,7,4}. \tag{127}$$

we obtain the following metric-dynamic model of the nucleus of the "hydrogen atom" in configuration (67).

CORE (128)

of the "hydrogen atom"

A spherical vacuum formation consisting of the cores of 2 “quarks” and 2 “antiquarks”:

The "electron’s" core (129)

signature $(+---)$

I $$ds_{1,2}^{(+---)2} = \left(1 + \frac{r_{S,2,1}}{r} - \frac{r^2}{r_6^2}\right) c^2dt^2 - \frac{dr^2}{\left(1 + \frac{r_{S,2,1}}{r} - \frac{r^2}{r_6^2}\right)} - r^2(d\theta^2 + \sin^2\theta\, d\phi^2), \quad (130)$$

H $$ds_{2,2}^{(,+---)2} = \left(1 - \frac{r_{S,2,2}}{r} + \frac{r^2}{r_6^2}\right) c^2dt^2 - \frac{dr^2}{\left(1 - \frac{r_{S,2,2}}{r} + \frac{r^2}{r_6^2}\right)} - r^2(d\theta^2 + \sin^2\theta\, d\phi^2), \quad (131)$$

V $$ds_{3,2}^{(+---)2} = \left(1 + \frac{r_{S,2,3}}{r} + \frac{r^2}{r_6^2}\right) c^2dt^2 - \frac{dr^2}{\left(1 + \frac{r_{S,2,3}}{r} - \frac{r^2}{r_6^2}\right)} - r^2(d\theta^2 + \sin^2\theta\, d\phi^2), \quad (132)$$

H′ $$ds_{4,2}^{(+---)2} = \left(1 - \frac{r_{S,2,4}}{r} - \frac{r^2}{r_6^2}\right) c^2dt^2 - \frac{dr^2}{\left(1 - \frac{r_{S,2,4}}{r} - \frac{r^2}{r_6^2}\right)} - r^2(d\theta^2 + \sin^2\theta\, d\phi^2); \quad (133)$$

The outer shell of the d_b^+-"quark" (134)

signature $(+-++)$

I $$ds_{1,4}^{(+-++)2} = \left(1 - \frac{r_{S,4,1}}{r} + \frac{r^2}{r_6^2}\right) c^2dt^2 - \frac{dr^2}{\left(1 - \frac{r_{S,4,1}}{r} + \frac{r^2}{r_6^2}\right)} + r^2d\theta^2 + r^2\sin^2\theta\, d\phi^2, \quad (135)$$

H $$ds_{2,4}^{(+-++)2} = \left(1 + \frac{r_{S,4,2}}{r} - \frac{r^2}{r_6^2}\right) c^2dt^2 - \frac{dr^2}{\left(1 + \frac{r_{S,4,2}}{r} - \frac{r^2}{r_6^2}\right)} + r^2d\theta^2 + r^2\sin^2\theta\, d\phi^2, \quad (136)$$

V $$ds_{3,4}^{(+-++)2} = \left(1 - \frac{r_{S,4,3}}{r} - \frac{r^2}{r_6^2}\right) c^2dt^2 - \frac{dr^2}{\left(1 - \frac{r_{S,4,3}}{r} - \frac{r^2}{r_6^2}\right)} + r^2d\theta^2 + r^2\sin^2\theta\, d\phi^2, \quad (137)$$

H′ $$ds_{4,4}^{(+-++)2} = \left(1 + \frac{r_{S,4,4}}{r} + \frac{r^2}{r_6^2}\right) c^2dt^2 - \frac{dr^2}{\left(1 + \frac{r_{S,4,4}}{r} + \frac{r^2}{r_6^2}\right)} + r^2d\theta^2 + r^2\sin^2\theta\, d\phi^2; \quad (138)$$

The outer shell of the u_r^--"quark" (139)

signature $(-++-)$

I $$ds_{1,6}^{(-++-)2} = -\left(1 - \frac{r_{S,6,1}}{r} + \frac{r^2}{r_6^2}\right) c^2dt^2 + \frac{dr^2}{\left(1 - \frac{r_{S,6,1}}{r} + \frac{r^2}{r_6^2}\right)} + r^2d\theta^2 - r^2\sin^2\theta\, d\phi^2, \quad (140)$$

H $$ds_{2,6}^{(-++-)2} = -\left(1 + \frac{r_{S,6,2}}{r} - \frac{r^2}{r_6^2}\right) c^2dt^2 + \frac{dr^2}{\left(1 + \frac{r_{S,6,2}}{r} - \frac{r^2}{r_6^2}\right)} + r^2d\theta^2 - r^2\sin^2\theta\, d\phi^2, \quad (141)$$

V $$ds_{3,6}^{(-++-)2} = -\left(1 - \frac{r_{S,6,3}}{r} - \frac{r^2}{r_6^2}\right) c^2dt^2 + \frac{dr^2}{\left(1 - \frac{r_{S,6,3}}{r} - \frac{r^2}{r_6^2}\right)} + r^2d\theta^2 - r^2\sin^2\theta\, d\phi^2, \quad (142)$$

H′ $$ds_{4,6}^{(-++-)2} = -\left(1 + \frac{r_{S,6,4}}{r} + \frac{r^2}{r_6^2}\right) c^2dt^2 + \frac{dr^2}{\left(1 + \frac{r_{S,6,4}}{r} + \frac{r^2}{r_6^2}\right)} + r^2d\theta^2 - r^2\sin^2\theta\, d\phi^2; \quad (143)$$

The outer shell of the u_g^--"quark" (144)

signature $(-+-+)$

I $$ds_{1,8}^{(-+-+)2} = -\left(1 - \frac{r_{S,8,1}}{r} + \frac{r^2}{r_6^2}\right) c^2dt^2 + \frac{dr^2}{\left(1 - \frac{r_{S,8,1}}{r} + \frac{r^2}{r_6^2}\right)} - r^2d\theta^2 + r^2\sin^2\theta\, d\phi^2, \quad (145)$$

H $$ds_{2,8}^{(-+-+)2} = -\left(1 + \frac{r_{S,8,2}}{r} - \frac{r^2}{r_6^2}\right) c^2dt^2 + \frac{dr^2}{\left(1 + \frac{r_{S,8,2}}{r} - \frac{r^2}{r_6^2}\right)} - r^2d\theta^2 + r^2\sin^2\theta\, d\phi^2, \quad (146)$$

V $$ds_{3,8}^{(--++)2} = -\left(1 - \frac{r_{S,8,3}}{r} - \frac{r^2}{r_6^2}\right) c^2dt^2 + \frac{dr^2}{\left(1 - \frac{r_{S,8,3}}{r} - \frac{r^2}{r_6^2}\right)} - r^2d\theta^2 + r^2\sin^2\theta\, d\phi^2, \quad (147)$$

H′ $$ds_{4,8}^{(-+-+)2} = -\left(1 + \frac{r_{S,8,4}}{r} + \frac{r^2}{r_6^2}\right) c^2dt^2 + \frac{dr^2}{\left(1 + \frac{r_{S,8,4}}{r} + \frac{r^2}{r_6^2}\right)} - r^2d\theta^2 + \sin^2\theta\, d\phi^2; \quad (148)$$

Adding up the metrics (130) – (133) + (135) – (138) + (140) – (143) + (145) – (148), we find that the outer, on average, spherical boundary of the c0re of the "hydrogen atom" with an average radius r_6 (127) contracts (or, more precisely, dissolves in the fluctuating vacuum).

As a result, when averaging from a set of metrics (128) (i.e., from a chaotically fluctuating vacuum), the outer shell (OS) of the inner (ioctoscopic, ~10^{-24} cm) nucleolus of the "electron" (i.e., the nucleolus of the e_y^+-"proto-quark") and the outer shells of the ioctoscopic nucleoli of the d_b^+-"proto-quark", u_r^--"proto-antiquark" and u_g^--"proto-antiquark" are revealed:

The outer shell (OS) of the inner (ioctoscope, ~10^{-24} cm) nucleolus
"ELECTRON" (149)
(or the OS of the e_y^+-"proto-quark's" nucleolus from the (62) hierarchy),
with the signature (+ – – –)

I $$ds_{1,2}^{(+---)2} = \left(1 + \frac{r_{S,2,1}}{r}\right) c^2dt^2 - \frac{dr^2}{\left(1 + \frac{r_{S,2,1}}{r}\right)} - r^2(d\theta^2 + \sin^2\theta\, d\phi^2), \quad (150)$$

H $$ds_{2,2}^{(,+---)2} = \left(1 - \frac{r_{S,2,2}}{r}\right) c^2dt^2 - \frac{dr^2}{\left(1 - \frac{r_{S,2,2}}{r}\right)} - r^2(d\theta^2 + \sin^2\theta\, d\phi^2), \quad (151)$$

V $$ds_{3,2}^{(+---)2} = \left(1 + \frac{r_{S,2,3}}{r}\right) c^2dt^2 - \frac{dr^2}{\left(1 + \frac{r_{S,2,3}}{r}\right)} - r^2(d\theta^2 + \sin^2\theta\, d\phi^2), \quad (152)$$

H′ $$ds_{4,2}^{(+---)2} = \left(1 - \frac{r_{S,2,4}}{r}\right) c^2dt^2 - \frac{dr^2}{\left(1 - \frac{r_{S,2,4}}{r}\right)} - r^2(d\theta^2 + \sin^2\theta\, d\phi^2); \quad (153)$$

The outer shell (OS) of the inner (ioctoscope-sized, ~10^{-24} cm) nucleolus (154)
"PROTON"
consisting of the OS of the inner nucleoli: a d_b^+-"quark" and two u_i^--"antiquarks,"
with a common signature (– + + +):

The OS of the d_b^+-"proto-quark" nucleolus (155)
with the signature (+ – + +)

I $$ds_{1,4}^{(+-++)2} = \left(1 - \frac{r_{S,4,1}}{r}\right) c^2dt^2 - \frac{dr^2}{\left(1 - \frac{r_{S,4,1}}{r}\right)} + r^2d\theta^2 + r^2\sin^2\theta\, d\phi^2, \quad (156)$$

H $$ds_{2,4}^{(+-++)2} = \left(1 + \frac{r_{S,4,2}}{r}\right) c^2dt^2 - \frac{dr^2}{\left(1 + \frac{r_{S,4,2}}{r}\right)} + r^2d\theta^2 + r^2\sin^2\theta\, d\phi^2, \quad (157)$$

V $$ds_{3,4}^{(+-++)2} = \left(1 - \frac{r_{S,4,3}}{r}\right) c^2dt^2 - \frac{dr^2}{\left(1 - \frac{r_{S,4,3}}{r}\right)} + r^2d\theta^2 + r^2\sin^2\theta\, d\phi^2, \quad (158)$$

H′ $$ds_{4,4}^{(+-++)2} = \left(1 + \frac{r_{S,4,4}}{r}\right) c^2dt^2 - \frac{dr^2}{\left(1 + \frac{r_{S,4,4}}{r}\right)} + r^2d\theta^2 + r^2\sin^2\theta\, d\phi^2; \quad (159)$$

The OS of the u_r^--"proto-quark" nucleolus (160)
with the signature (– + + –)

I $$ds_{1,6}^{(-++-)2} = -\left(1 - \frac{r_{S,6,1}}{r}\right) c^2dt^2 + \frac{dr^2}{\left(1 - \frac{r_{S,6,1}}{r}\right)} + r^2d\theta^2 - r^2\sin^2\theta\, d\phi^2, \quad (161)$$

H $$ds_{2,6}^{(-++-)2} = -\left(1 + \frac{r_{S,6,2}}{r}\right) c^2dt^2 + \frac{dr^2}{\left(1 + \frac{r_{S,6,2}}{r}\right)} + r^2d\theta^2 - r^2\sin^2\theta\, d\phi^2, \quad (162)$$

V $$ds_{3,6}^{(-++-)2} = -\left(1 - \frac{r_{S,6,3}}{r}\right) c^2dt^2 + \frac{dr^2}{\left(1 - \frac{r_{S,6,3}}{r}\right)} + r^2d\theta^2 - r^2\sin^2\theta\, d\phi^2, \quad (163)$$

H′ $$ds_{4,6}^{(-++-)2} = -\left(1 + \frac{r_{S,6,4}}{r}\right) c^2dt^2 + \frac{dr^2}{\left(1 + \frac{r_{S,6,4}}{r}\right)} + r^2d\theta^2 - r^2\sin^2\theta\, d\phi^2; \quad (164)$$

The OS of the u_g^--"proto-quark" nucleolus (165)
with the signature (– + – +)

I $$ds_{1,8}^{(-+-+)2} = -\left(1 - \frac{r_{S,8,1}}{r}\right) c^2dt^2 + \frac{dr^2}{\left(1 - \frac{r_{S,8,1}}{r}\right)} - r^2d\theta^2 + r^2\sin^2\theta\, d\phi^2, \quad (166)$$

H $$ds_{2,8}^{(-+-+)2} = -\left(1 + \frac{r_{S,8,2}}{r}\right) c^2dt^2 + \frac{dr^2}{\left(1 + \frac{r_{S,8,2}}{r}\right)} - r^2d\theta^2 + r^2\sin^2\theta\, d\phi^2, \quad (167)$$

V $$ds_{3,8}^{(--++)2} = -\left(1-\frac{r_{S,8,3}}{r}\right)c^2dt^2 + \frac{dr^2}{\left(1-\frac{r_{S,8,3}}{r}\right)} - r^2d\theta^2 + r^2\sin^2\theta\, d\phi^2, \quad (168)$$

H′ $$ds_{4,8}^{(-+-+)2} = -\left(1+\frac{r_{S,8,4}}{r}\right)c^2dt^2 + \frac{dr^2}{\left(1+\frac{r_{S,8,4}}{r}\right)} - r^2d\theta^2 + \sin^2\theta\, d\phi^2; \quad (169)$$

where the radii of the "flow quarks" and "proto-antiquarks" nuclei are significantly less than 10^{-17}cm

(170)

$$r_{S,2,1} \approx r_{S,2,2} \approx r_{S,2,3} \approx r_{S,2,4} \approx r_{S,4,1} \approx r_{S,4,2} \approx r_{S,4,3} \approx r_{S,4,4} \approx r_{S,6,1} \approx r_{S,6,2} \approx r_{S,6,3} \approx r_{S,6,4} \approx r_{S,8,1} \approx r_{S,8,2} \approx r_{S,8,3} \approx r_{S,8,4} \ll \mathbf{10^{-17}}\text{m}$$

We note once again that the hierarchical sequence of radii (62) provides an estimate of the radius of the "proto-quark's" nucleolus $r_7 \sim 10^{-24}$ cm, but this has not been confirmed experimentally. Therefore, a more conservative estimate of $r_7 \approx r_{S,ij} \ll 10^{-17}$ cm is used here. For this article, this estimate is sufficient, since the sizes of the nuclei of the "proto-quarks" have practically no effect on the further presentation; it is only important that they are several orders of magnitude smaller than 10^{-13} cm.

4. A simplified metrico-dynamic model of the "hydrogen atom"

Let us perform another step of pairwise averaging of the sets of metrics (150) – (153), (156) – (159), (161) – (164), and (166) – (169). As a result, assuming approximate equality of all $r_{S,i,j} \approx r_7 \ll 10^{-17}$ cm (170) and, on average, the zero state of the outer shell of the "hydrogen atom," as described in §2, we obtain the following simplified metrico-dynamic model of the "hydrogen atom."

The averaged contours of the metric-dynamic model of a stationary

H_1^+-"HYDROGEN ATOM" (171)

revealed from a chaotically fluctuating vacuum,

with a common signature (0 0 0 0), consisting of:

The outer shell of the inner nucleolus

"ELECTRON" (172)

(i.e., the outer shell of the e_y^+-"proto-quark's" nucleolus),

with a signature (+ – – –)

I $$ds_{1,2}^{(+---)2} = \left(1+\frac{r_7}{r}\right)c^2dt^2 - \frac{dr^2}{\left(1+\frac{r_7}{r}\right)} - r^2(d\theta^2 + \sin^2\theta\, d\phi^2), \quad (173)$$

H $$ds_{2,2}^{(,+---)2} = \left(1-\frac{r_7}{r}\right)c^2dt^2 - \frac{dr^2}{\left(1-\frac{r_7}{r}\right)} - r^2(d\theta^2 + \sin^2\theta\, d\phi^2), \quad (174)$$

The substrate of the "electron"

в интервале [0, ∞], с сигнатурой (– + + +)

i $$ds_{5.1}^{(+---)2} = c^2dt^2 - dr^2 - r^2(d\theta^2 + \sin^2\theta\, d\phi^2);$$

The outer shell (OS) of the internal nucleolus

"PROTON" (175)

consisting of the OS of a internal nucleoli of the: d_r^+-"quark" and two u_i^--"antiquarks",

with a common signature (– + + +):

The OS of the nucleolus d_b^+-"proto-quark" (176)

with signature (+ – + +)

I $$ds_{1,4}^{(+-++)2} = \left(1-\frac{r_7}{r}\right)c^2dt^2 - \frac{dr^2}{\left(1-\frac{r_7}{r}\right)} + r^2d\theta^2 + r^2\sin^2\theta\, d\phi^2, \quad (177)$$

H $$ds_{2,4}^{(+-++)2} = \left(1+\frac{r_7}{r}\right)c^2dt^2 - \frac{dr^2}{\left(1+\frac{r_7}{r}\right)} + r^2d\theta^2 + r^2\sin^2\theta\, d\phi^2, \quad (178)$$

The OS of the nucleolus u_r^--"proto-antiquark" (179)

with signature (– + + –)

I $$ds_{1,6}^{(-++-)2} = -\left(1 - \frac{r_7}{r}\right) c^2 dt^2 + \frac{dr^2}{\left(1 - \frac{r_7}{r}\right)} + r^2 d\theta^2 - r^2 \sin^2\theta\, d\phi^2, \quad (180)$$

H $$ds_{2,6}^{(-++-)2} = -\left(1 + \frac{r_7}{r}\right) c^2 dt^2 + \frac{dr^2}{\left(1 + \frac{r_7}{r}\right)} + r^2 d\theta^2 - r^2 \sin^2\theta\, d\phi^2; \quad (181)$$

The OS of the nucleolus u_g^--"proto-antiquark" (182)

with signature (– + – +)

I $$ds_{1,8}^{(-+-+)2} = -\left(1 - \frac{r_7}{r}\right) c^2 dt^2 + \frac{dr^2}{\left(1 - \frac{r_7}{r}\right)} - r^2 d\theta^2 + r^2 \sin^2\theta\, d\phi^2, \quad (183)$$

H $$ds_{2,8}^{(-+-+)2} = -\left(1 + \frac{r_7}{r}\right) c^2 dt^2 + \frac{dr^2}{\left(1 + \frac{r_7}{r}\right)} - r^2 d\theta^2 + r^2 \sin^2\theta\, d\phi^2; \quad (184)$$

The substrate of the "proton"

в интервале [0, ∞], с сигнатурой (– + + +)

i $$ds_{5.1}^{(-+++)2} = -c^2 dt^2 + dr^2 + r^2(d\theta^2 + \sin^2\theta\, d\phi^2). \quad (185)$$

As a result, we arrive at the following simplified model of the "hydrogen atom". From a chaotically fluctuating vacuum, when averaging a set of metrics (72), the core of a "hydrogen atom" with a conditional effective radius r_{eff} ~10^{-13} cm (see Figure 6 and 7) is revealed, which is formed as a result of complex (chaotic) movements and intertwining of interconnected nucleoli d_i^+- "proto-quark" and two u_j^--"proto-antiquarks" (see Figure 6). Separately, these nucleoli of a "proto-quark" and 2 "proto-antiquarks" cannot exist, because are convex-concave (unstable) vacuum states with signatures (i.e., topologies) indicated in the numerators of the rankings (31) – (33). Only together they form, on average, a concave spherical vacuum formation with a common (average) signature (– + + +) and with an effective radius r_{eff} ~10^{-13} cm. Moreover, these nucleoli of a "proto-quark" and two "proto-antiquarks" constantly move chaotically relative to the center of this formation (i.e., topological node) and relative to each other (see Figure 7) and continuously change the topological (signature) configuration, i.e., constantly undergo metamorphoses, for example, from (31) → (32) → (31) → (33) → (32) →… etc. (see Figure 6).

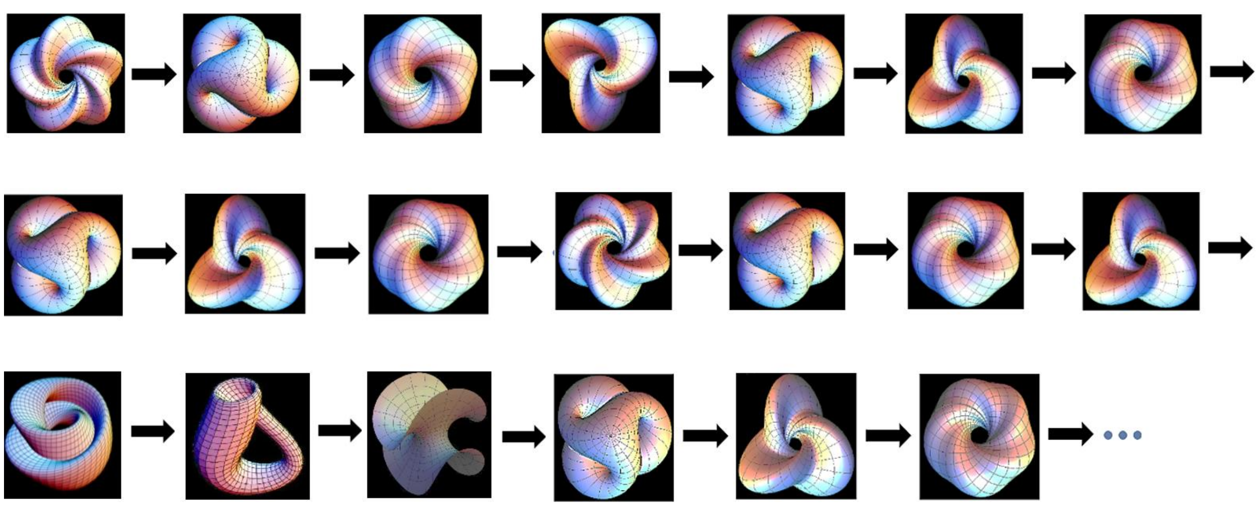

Fig. 6: Illustration of a constant change in the topological (signature) node of 3 connected "proto-quark's" nucleoli

In addition to the "hydrogen atom" (175) identified from the chaos of the outer shell of the nucleus (see Figure 7), also from the chaotically fluctuating vacuum, when averaging a set of metrics (72), another stable spherical vacuum formation is revealed – this is the internal nucleolus of the "electron" (i.e., the nucleolus of the e_y^+-"proto-quark"), with an effective radius of the order of $r_7 \ll 10^{-17}$ cm s outer shell (173) – (174) (see Figure 7 and Figure 14 in [7]).

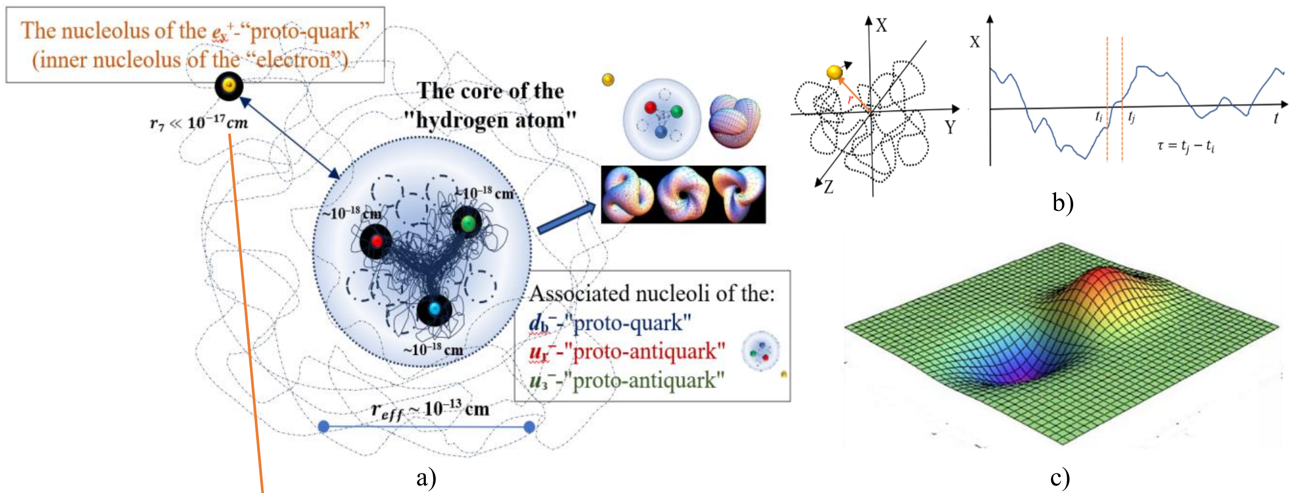

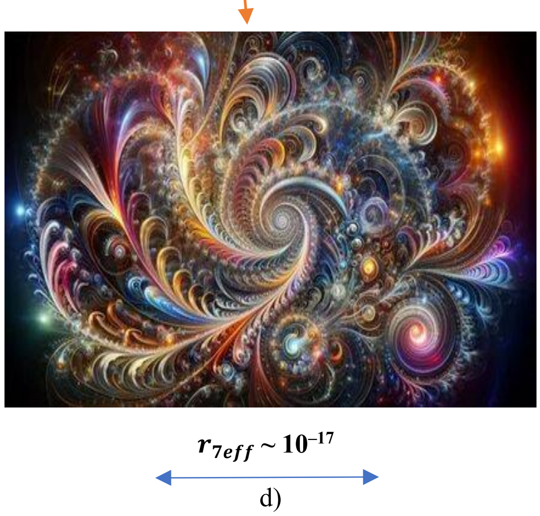

Fig. 7: a) A simplified schematic model of the "hydrogen atom", consisting of an internal nucleolus of an "electron" with a radius $r_7 \ll 10^{-17}$ cm and a core of this "atom" with an effective radius $r_{eff} \sim 10^{-13}$ cm, formed by a complex interweaving of internal nucleoli of 3 valence "quarks" and "antiquarks" in configuration (33) and 6 virtual "quarks" and "antiquarks" in configurations (31) and (32). These internal nucleoli (i.e., the nuclei of a "proto-quark" and 2 "proto-antiquarks") constantly move chaotically relative to each other and are continuously transformed into other triplets of internal nucleoli "proto-quarks" and "proto-antiquarks" (31) and (32). At the same time, the internal nucleolus of the "electron" (i.e., the nucleolus of the e_y^+-"proto-quark") with a radius $r_{7eff} \ll 10^{-17}$ cm continuously chaotically moves around this "atom's" core; b) Chaotic trajectory of the nucleolus of the e_y^+-"proto-quark" in the vicinity of the core of the "hydrogen atom" and its projection on the X axis; c) Two-dimensional illustration of the movement of the nucleolus e_y^+-"proto-quark" (i.e., a spherical 3-dimensional convexity of vacuum with a signature (+ – – –)) around the core of an "atom" (i.e., a stable on average spherical 3-dimensional concavity of vacuum with an average signature (– + + +)); d) Fractal illustration of the effective size of the nucleolus of the e_y^+-"proto-quark", which, together with its nearest outer shell, moves as a single whole in the vicinity of the effective core of the "hydrogen atom" along a chaotic trajectory

5. Electron-proton interaction within a "hydrogen atom"

In the previous paragraph, it was shown that at the location of the hydrogen atom, when simplifying and averaging the set of metrics (72), two stable spherical vacuum formations emerge from the chaotically fluctuating vacuum:

1) the convex nucleolus of the e_y^+-"proto-quark" (see Figure 7) with a metric-dynamic model of its outer shell

The outer shell of the convex nucleolus of the e_y^+-"proto-quark" (186)
with signature (+ – – –)

I $$ds_{1,2}^{(+---)2} = \left(1+\frac{r_7}{r}\right)c^2dt^2 - \frac{dr^2}{\left(1+\frac{r_7}{r}\right)} - r^2(d\theta^2 + \sin^2\theta\, d\phi^2), \quad (187)$$

H $$ds_{2,2}^{(,+---)2} = \left(1-\frac{r_7}{r}\right)c^2dt^2 - \frac{dr^2}{\left(1-\frac{r_7}{r}\right)} - r^2(d\theta^2 + \sin^2\theta\, d\phi^2), \quad (188)$$

i $$ds_{5.1}^{(+---)2} = c^2dt^2 - dr^2 - r^2(d\theta^2 + \sin^2\theta\, d\phi^2). \quad (189)$$

2) the concave core of the "hydrogen atom" (i.e., the seething and bubbling internal nucleolus of the "proton", see Figures 6 and 7) with an averaged metric-dynamic model of its outer shell (175), which, at a sufficiently large distance from the center of this nucleus (i.e., at $r \gg 10^{-13}$ cm), is the result of averaging metrics (177) − (184).

The outer shell of the concave core of the "hydrogen atom" (190)

at $r \gg 10^{-13}$ см cm, with signature $(-+++)$:

I $$ds_1^{(-+++)2} = -\left(1 - \frac{r_{eff}}{r}\right) c^2dt^2 + \frac{dr^2}{\left(1 - \frac{r_{eff}}{r}\right)} + r^2 d\theta^2 + r^2 \sin^2\theta \, d\phi^2, \tag{191}$$

H $$ds_2^{(-+++)2} = -\left(1 + \frac{r_{eff}}{r}\right) c^2dt^2 + \frac{dr^2}{\left(1 + \frac{r_{eff}}{r}\right)} + r^2 d\theta^2 - r^2 \sin^2\theta \, d\phi^2, \tag{192}$$

i $$ds_{5.1}^{(-+++)2} = -c^2dt^2 + dr^2 + r^2(d\theta^2 + \sin^2\theta \, d\phi^2), \tag{193}$$

where $r_{eff} \sim 10^{-13}$cm is the effective radius of the "hydrogen atom's" core (see Figure 6a).

The interaction of two (convex and concave) stable vacuum formations with outer shells (186) and (190) is discussed in detail in §§2 and 10 in [7].

If we repeat the same reasoning and calculations that were performed in the article [7], then, based on metrics (187) – (189), we obtain that the e_y^+-"proto-quark's" nucleus attracts the "hydrogen atom" nucleus with acceleration

$$a_r^{(e+P)} \approx \frac{c^2 r_7}{2r^2\sqrt{\left(1 - \frac{r_7^2}{r^2}\right)}}, \quad \text{where according to the hierarchy of radii (62) } r_7 \sim 10^{-24}\text{cm} \ll 10^{-17}\text{cm}. \tag{194}$$

Similarly, based on metrics (191) – (193), we obtain that the core of the "hydrogen atom" attracts the nucleolus of the yellow e_y^+-"proto-quark" with acceleration

$$a_r^{(P+e)} \approx \frac{v_e^2 r_{eff}}{2r^2\sqrt{\left(1 - \frac{r_{eff}^2}{r^2}\right)}}, \tag{195}$$

where v_e is the speed of the average vacuum flow, which will be defined below.

$$a_r^{(e,P)} = a_r^{(e+P)} + a_r^{(P+e)} \approx \frac{c^2 r_7}{2r^2\sqrt{\left(1 - \frac{r_7^2}{r^2}\right)}} + \frac{v_e^2 r_{eff}}{2r^2\sqrt{\left(1 - \frac{r_{eff}^2}{r^2}\right)}}, \tag{196}$$

where r is the distance between the centers of the core of the "atom" and the e_y^+-"proto-quark" nucleus.
Since r_{eff} is several orders of magnitude greater than r_7 (i.e., $r_{eff} \gg r_7$), the first term in expression (196) can be neglected. Then, the acceleration of convergence (196) of the vacuum formations under consideration takes the approximate form

$$a_r^{(e,P)}(r) \approx \frac{v_e^2 r_{eff}}{2r^2\sqrt{\left(1 - \frac{r_{eff}^2}{r^2}\right)}}. \tag{197}$$

The graph of function (197) is shown in Figure 8. This function determines the acceleration of the approach of the e_y^+-"proto-quark's" core to the "hydrogen atom's" core (essentially, the "proton's" core) depending on the distance r between their centers.

From the graph in Figure 7, it is clear that the e_y^+-"proto-quark's" nucleolus can approach the "hydrogen atom's" core at no more than a distance

$r \approx r_{eff} \sim 10^{-13} cm.$ (198)

That is, under normal conditions, the nucleolus of the e_y^+-“proto-quark” practically does not penetrate into the nucleus of the “hydrogen atom”.

But raqiya (i.e., an abyss-crack, see Figure 1 in [7]) at a distance $r \approx r_{eff} \sim 10^{-13}$cm is absent in this case. The question arises: - What prevents the nucleolus of the e_y^+-“proto-quark” from ending up in the center of the “hydrogen atom”?

This is prevented by the outer shell of the nucleolus d_b^+-“proto-quark” (176), which has the same electric charge (i.e., the same first positive sign in the signature) as the outer shell of the nucleolus e_y^+-“proto-quark” (186). In other words, at small distances between the nuclei of these vacuum formations (i.e., at $r \leq r_{eff}$), the outer shell of the d_b^+-“proto-quark” noticeably pushes the nucleolus of the e_y^+-“proto-quark” away from itself, thereby pushing it out of the center of the core of the “hydrogen atom”. For $r \gg r_{eff}$ Ex. (197) is simplified

$$a_r^{(e,P)}(r) \approx \frac{v_e^2 r_{eff}}{2r^2}, \qquad (199)$$

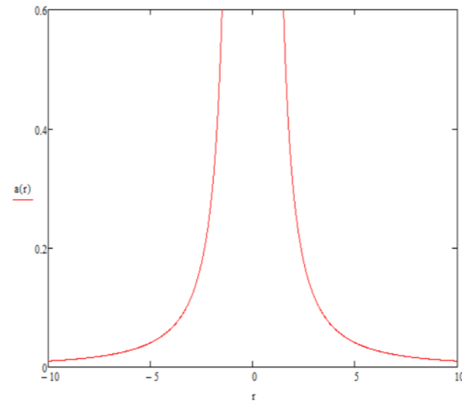

Fig. 8: Graph of the acceleration function (197) for the conventionally accepted $c = r_{eff} = 1$. This function determines the acceleration of the approach of the e_y^+-“proto-quark’s” nucleus to the “hydrogen atom’s” core (i.e., to the “proton” nucleus) depending on the distance between their centers

and corresponds to the average strength of the pseudo-Coulomb interaction between the nucleus of the e_y^+-“proto-quark” and the core of the “hydrogen atom”.

6. Transmutation of a "hydrogen atom" into a "neutron"

Since there is no raqiya (i.e., an insurmountable spherical abyss-crack) at a distance of $r \approx r_{eff} \sim 10^{-13}$ cm around the hypothetical core of a "hydrogen atom," the question arises of whether it is possible to press the e_y^+-"proto-quark’s" nucleolus into this core. That is, to create a pressure on the e_y^+-"proto-quark’s" nucleolus that overcomes the repulsion from the outer shell of the d_b^+-"proto-quark".

This is apparently possible. Most likely, this involves a transmutation (i.e., a topological rearrangement) of the "hydrogen atom" into a "neutron," for example:

(200)

$$\boxed{\text{«neutron» (53a)}} \quad \begin{matrix}(-\;-\;-\;-)\\(+\;-\;+\;+)\\(-\;+\;+\;-)\\ \underline{(+\;+\;-\;+)}\\(0\;\;0\;\;0\;\;0)_+\end{matrix} \;\leftarrow\; \begin{matrix}(+\;-\;+\;+)\\(-\;+\;+\;-)\\(-\;+\;-\;+)\\ \underline{(+\;-\;-\;-)}\\(0\;\;0\;\;0\;\;0)_+\end{matrix} \begin{matrix} \leftarrow \boxed{p_i^-\text{-«proton» (33)}} \\ \leftarrow \boxed{\text{«electron» (11)}}\end{matrix}$$

This possibility is consistent with the theoretical basis for the existence of neutron stars. It is believed that at the end of a sufficiently massive star's life, its nuclear fuel burns out, and under the influence of strong gravity, protons and electrons are "squeezed" into each other, turning into neutrons and emitting neutrinos. It is reasonably assumed that the numerous radio pulsars, magnetars, and *X*-ray pulsars discovered are varieties of real neutron stars.

7. Equation for describing the chaotic behavior of the $e_ж^+$-“proto-quark’s” nucleolus in the vicinity of the “hydrogen atom’s” core

As shown in [13,14], the time-invariant averaged behavior (state) of a randomly wandering particle (RWP) (in particular, the $e_ж^+$-“proto-quark’s” nucleolus (ePQN) chaotically moving in the vicinity of the “hydrogen atom’s” core, (see Figure 7) is described by the stochastic massless stationary Schrödinger equation (132) in [13]

$$-\frac{3\eta_r^2}{4}\nabla^2\phi(r)+u(r)\phi(r)=\varepsilon\phi(r), \quad (201)$$

where

$\phi(r)$ is the probability amplitude such that $|\phi(r)|^2=\rho(r)$ is the probability density function of the location of a chaotically wandering particle (ChWP) (in particular, a of the $e_ж^+$-"proto-quark's" nucleolus (ePQN)); (202)

$\varepsilon=\frac{E}{m_e}$ is the total mechanical energetics of the chaotically wandering ePQN (see Figure 7b) (where E is the total mechanical energy of the ePQN particle, m_e is the particle mass); (203)

$u(r)=\frac{U(r)}{m_e}$ is the average potential energetics of the chaotically wandering ePQN, depending on its distance r from the center of the "hydrogen atom's" core (where $U(r)$ is the average potential energy of the ePQN); (204)

$\sigma_r=\frac{1}{3}(\sigma_x+\sigma_x+\sigma_x)\approx\sigma_x$ (205)

is standard deviation of the 3-dimensional chaotic trajectory of the chaotically wandering ePQN (see Figure 7b);

$\tau_{racor}=\frac{1}{3}\left(\tau_{xacor}+\tau_{yacor}+\tau_{zacor}\right)\approx\tau_{xacor}$ (206)

is autocorrelation interval of the 3-dimensional chaotic trajectory of the chaotically wandering ePQN (see Figure 7b).

As is well known, the stationary Schrödinger equation has the form

$$-\frac{\hbar^2}{2m_e}\nabla^2\psi(r)+U(r)\psi(r)=E\psi(r), \quad (207)$$

where $\psi(r)$ is the wave function.

Dividing both sides of this equation by the particle mass m_e, we obtain

$$-\frac{\hbar^2}{2m_e^2}\nabla^2\psi(r)+u(r)\psi(r)=\varepsilon\psi(r). \quad (208)$$

Obviously, for $\phi(r)=\psi(r)$ and

$$\frac{\hbar}{m_e}=\sqrt{\frac{3}{2}}\eta_r=\sqrt{\frac{3}{2}}\frac{\sigma_r^2}{\tau_{rcor}} \quad (209)$$

stochastic equation (201) and quantum mechanical equation (208) coincide.

8. Chaotic behavior of the e_y^+-"proto-quark's" nucleolus near the core of a "hydrogen atom"

In §7, it was shown that the e_y^+-"proto-quark's" nucleolus (ePQN), constantly wandering chaotically near the core of a "hydrogen atom," is, on average, attracted to this core with an acceleration (199)

$$a_r^{(e,P)}(r)\approx\frac{v_e^2r_{eff}}{2r^2}, \quad (210)$$

In this case, the average potential energetics of the chaotically wandering ePQN

$$u(r)=\frac{U(r)}{m_e}\approx\int a_r^{(e,P)}(r)dr=\int\frac{v_e^2r_{eff}}{r^2}dr=-\frac{v_e^2r_{eff}}{2r}. \quad (211)$$

Substituting Ex. (211) into Eq. (201) yields the stochastic equation

$$\left[-\frac{3\eta_r^2}{4}\nabla^2-\frac{v_e^2r_{eff}}{2r}\right]\phi(r)=\varepsilon\phi(r), \quad (212)$$

which coincides, up to coefficients, with the stationary Schrödinger equation for the motion of an electron in a hydrogen atom:

$$\left[-\frac{\hbar^2}{2m_e^2}\nabla^2 - \frac{e^2}{4\pi m_e \varepsilon_0 r}\right]\psi(r) = \varepsilon\psi(r). \tag{213}$$

Comparing equations (212) and (213), we find that for $\phi(r) = \psi(r)$, we obtain the approximate equalities

$$\frac{v_e^2 r_{eff}}{2} \approx \frac{e^2}{4\pi m_e \varepsilon_0} \quad \text{and} \quad \frac{\hbar}{m_e} \approx \sqrt{\frac{3}{2}}\eta_r = \sqrt{6}\frac{\sigma_r^2}{\tau_{rcor}},$$

from which we can estimate the parameters v_e and η_r

$$v_e \approx \sqrt{\frac{e^2}{2\pi m_e \varepsilon_0 r_{eff}}} \approx \sqrt{\frac{2.56\cdot10^{-38}}{2\cdot3.14\cdot9.1\cdot10^{-31}\cdot8.85\cdot10^{-12}\cdot10^{-13}}} \approx \sqrt{\frac{2.56\cdot10^{-38}}{0.5\cdot10^{-53}}} \approx \sqrt{51.2\cdot10^{14}} = 7.2\cdot10^{7}\ \text{м/с}, \tag{214}$$

$$\eta_r = \frac{2\sigma_r^2}{\tau_{rcor}} = \sqrt{\frac{2}{3}}\frac{\hbar}{m_e} \approx 0{,}58\ \frac{1{,}05\cdot10^{-34}}{9{,}1\cdot10^{-31}} \approx 9.4\cdot10^{-5}\ \text{м}^2/\text{с}. \tag{215}$$

The Bohr radius of the electron orbit in a hydrogen atom can also be expressed through the stochastic characteristics of the random process under study, associated with a chaotically wandering e_y^+-"proto-quark's" nucleolus (ePQN) in the vicinity of the "hydrogen atom's" core (see Figure 7).

$$a_0 = \frac{4\pi\varepsilon_0\hbar^2}{m_e e^2} = \frac{4\pi m_e \varepsilon_0 \hbar^2}{m_e^2 e^2} \approx \frac{12\sigma_r^4}{v_e^2 r_{eff}\tau_{rcor}^2} \approx 5.29\cdot10^{-9}\ \text{cm}. \tag{216}$$

Solutions to equations of the form (212) in spherical coordinates are well known in quantum mechanics and have the form

$$a_0 = \frac{4\pi\varepsilon_0\hbar^2}{m_e e^2} = \frac{4\pi m_e \varepsilon_0 \hbar^2}{m_e^2 e^2} \approx \frac{12\sigma_r^4}{v_e^2 r_{eff}\tau_{rcor}^2} \approx 5.29\cdot10^{-9}\ \text{cm}. \tag{216}$$

Solutions of equations of the form (212) in spherical coordinates are well known in quantum mechanics and have the form

$$\phi(r)_{nlm}(r,\theta,\varphi) = R_{nl}(r)\,Y_{lm}(\theta,\varphi), \tag{217}$$

$$R_{nl}(r) = \sqrt{\left(\frac{2}{na_0}\right)^3 \frac{(n-l-1)!}{2n[(n+l)!]^3}}\left(\frac{2r}{na_0}\right)^l L_{n-l-1}^{2l+1}\left(\frac{2r}{na_0}\right)e^{-r/(na_0)} \text{ is normalized radial function;} \tag{218}$$

$L_{n-l-1}^{2l+1}(x)$ is generalized Laguerre polynomials;

$n = 0,1,2,\ldots$ is principal quantum number;

$l = 0,1,2,\ldots$ is orbital quantum number;

m – magnetic quantum number;

$$Y_{lm}(\theta,\varphi) = \begin{cases} \sqrt{\frac{2l+1}{4\pi}}P_l^0(cos\theta) & for\ m = 0 \\ (-1)^m\sqrt{2}\sqrt{\frac{2l+1}{4\pi}\frac{(l-m)!}{(l+m)!}}P_l^m(cos\theta)\cos(m\varphi) & for\ m > 0 \end{cases} \quad \text{are spherical harmonics,} \tag{219}$$

where $P_l^m(cos\theta)$ is the associative Legendre function with the Condon–Shortley phase.

Figure 9a shows the results of substitutions of various sets of quantum numbers *n, l, m* into Ex. (217). Graphs of some wave functions $\phi(r)_{nlm} = \psi(r)_{nlm}$ are shown in Figure 9b.

$n=1,\ l=0,\ m=0$	$\phi(r)_{100} = \frac{1}{\sqrt{\pi a_0^3}} e^{-r/a_0}$ (220)
$n=2,\ l=0,\ m=0$	$\phi(r)_{200} = \frac{1}{4\sqrt{\pi a_0^3}} \left(2 - \frac{r}{a_0}\right) e^{-r/2a_0}$
$n=2,\ l=1,\ m=0$	$\phi(r)_{210} = \frac{1}{4\sqrt{\pi a_0^3}} \frac{r}{a_0} e^{-r/2a_0} cos\theta$
$n=2,\ l=1,\ m=+1$	$\phi(r)_{211} = \frac{1}{4\sqrt{\pi a_0^3}} \frac{r}{a_0} e^{-r/2a_0} sin\varphi cos\theta$
$n=2,\ l=1,\ m=-1$	$\phi(r)_{21-1} = \frac{1}{4\sqrt{\pi a_0^3}} \frac{r}{a_0} e^{-r/2a_0} sin\varphi sin\theta$

а)

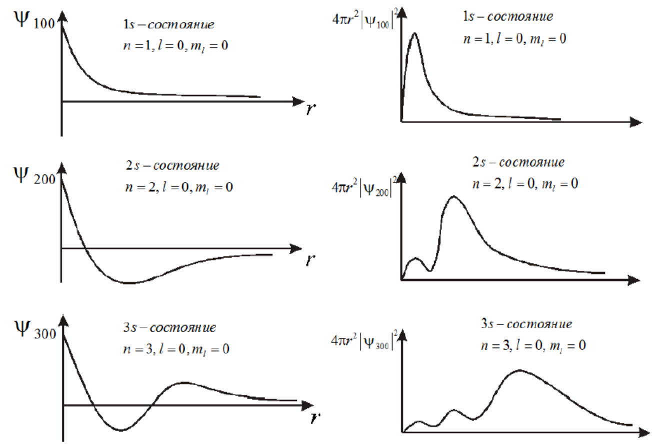

б) в)

Fig. 9: a) Wave functions of the chaotically wandering ePQN in the "hydrogen atom" $\phi(r)_{n,l,m}$ upon substituting different values of the quantum numbers *n, l, m* into Ex. (217); b) Graphs of three wave functions $\phi(r)_{n,l,m} = \psi(r)_{nlm}$ (217); c) Distribution densities of the probability $4\pi r^2 \left|\phi(r)_{n,l,m}\right|^2$ that the ePQN is located in a spherical layer $4\pi r^2 dr$

From the graphs of the functions $\phi(r)_{n,l,m} = \psi(r)_{nlm}$ (217) in Figure 9b, it is evident that in these states, the nucleolus of the e_y^+-"proto-quark" (ePQN) is more likely to be found at the center of the "hydrogen atom." This contradicts the assertion that the outer shell of the nucleolus of the d_b^+-"proto-quark" at short distances, on average, pushes the ePQN out of the center of the "hydrogen atom" nucleus (see §5). In other words, within the framework of the stochastic metric-dynamic model developed here, the probability of the appearance of a ePQN at the center of the "hydrogen atom's" core should be minimal.

Apparently, the creators of the quantum mechanical model of the hydrogen atom also understood that the center of this atom is the least likely place for an electron to appear. More precisely, they knew from the works of Niels Bohr that an electron in the ground state is most likely to be found in the region of the Bohr radius $a_0 = \frac{4\pi\varepsilon_0\hbar^2}{m_e e^2} \approx 5.29 \cdot 10^{-9}$ *cm." Therefore, in quantum mechanics (QM), the observable quantity is considered to be the probability density function* $4\pi r^2 \left|\phi(r)_{n,l,m}\right|^2$ *of detecting an electron in a spherical layer between a sphere with radius r and a sphere with radius r+dr. The graphs of these probability densities are shown in Figure 9c. However, this formal mathematical approach appears insufficiently convincing. In this case, the probability of finding an electron at the center of the nucleus decreases not due to the essential wave function* $\phi(r)_{n,l,m}$*, but due to the decrease in the volume of the spherical layer as it approaches the center of the atom's nucleus. Within the neopositivist ideology of the Copenhagen school, this formal mathematical approach is justified by the fact that, in their view, the electron has neither a trajectory nor a size. They conceive of the electron not as a particle, but as a kind of electron cloud. Therefore, it is easy to imagine that, in percentage terms, the center of the nucleus contains less of this cloud than the Bohr orbit.*

Within the framework of the statistical metric-dynamic model of the "hydrogen atom" developed here, the chaotically wandering nucleolus of the e_y^+-"proto-quark" (ePQN) has a quite noticeable effective size of $r_{7eff} \sim 10^{-17}$cm (see Figures 7d и 11) and a complex trajectory of motion (see Figure 7b). In this case, one must take into account the actual, rather than formal, expulsion of the ePQN from the center of the "atom's" core by the outer shell of the d_b^+-"proto-quark's" nucleolus.

To solve this problem, it is proposed to determine the average potential energy $u(r)$ of the chaotically wandering ePQN inside the "hydrogen atom" not based on the simplified acceleration (210), but on the more precise expression (197) for distances $|\ r_{eff}\ | < |\ r\ |$

$$u_{\text{eff}}(r) = \frac{U(r)}{m_e} \approx \int a_r^{(e,P)}(r)dr = \int \frac{v_e^2 r_{eff}}{2r^2\sqrt{\left(1-\frac{r_{eff}^2}{r^2}\right)}} dr = -\frac{v_e^2}{2} \arcsin\left(\frac{r_{eff}}{r}\right). \qquad (221)$$

The graph of this function, assuming $v_e = r_{eff} = 1$, is shown in Figure 10b.

In this case, the stochastic Schrödinger equation (201) for the e_y^+-"proto-quark's" nucleus (ePQN), randomly wandering in the vicinity of the "hydrogen atom's" core, takes the form

$$\left[-\frac{3\eta_r^2}{4}\nabla^2 - \frac{v_e^2}{2}\arcsin\left(\frac{r_{eff}}{r}\right)\right]\phi(r) = \varepsilon\phi(r), \tag{222}$$

or $$\nabla^2\phi(r) + \frac{4}{3\eta_r^2}\left(\varepsilon + \frac{v_e^2}{2}\arcsin\left(\frac{r_{eff}}{r}\right)\right)\phi(r) = 0, \tag{223}$$

and also, in the version of quantum mechanics

$$\nabla^2\psi(r) + \frac{2m_e^2}{\hbar^2}\left(\varepsilon + \frac{v_e^2}{2}\arcsin\left(\frac{r_{eff}}{r}\right)\right)\psi(r) = 0. \tag{224}$$

Solving Eq. (223) (or (224)) requires a separate study. This could potentially allow for effects such as the Lamb shift and other radiative corrections to the fine structure of the hydrogen atom to be taken into account without resorting to perturbation theory.

However, it can already be noted that for $r \gg r_{eff}$

$$-\frac{v_e^2}{2}\arcsin\left(\frac{r_{eff}}{r}\right) \approx -\frac{v_e^2 r_{eff}}{2r}. \tag{225}$$

This is evident from the graphs of these functions (see Figure 10), as well as from the fact that acceleration (197) at $r \gg r_{eff}$ is approximately equal to acceleration (198).

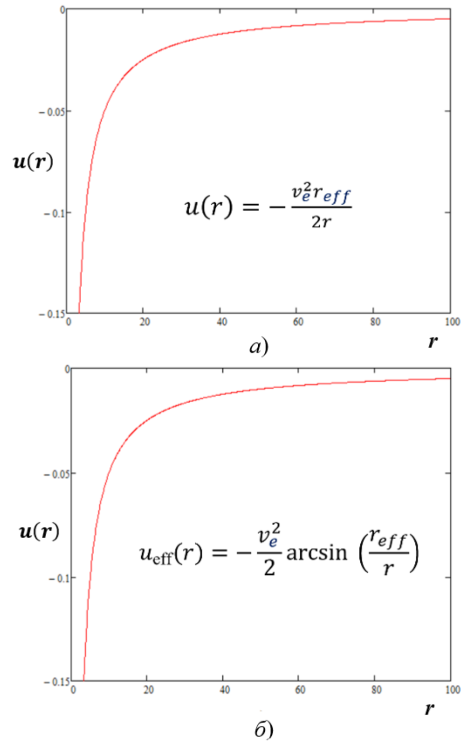

Fig. 10: a) Graph of the function $u(r)$ (211) with conditionally accepted $v_e = r_{eff} = 1$;
b) Graph of the function $u(r)$ (221) with conditionally accepted $v_e = r_{eff} = 1$

Therefore, for ePQN located at large distances from the "hydrogen atom's" core (for example, at distances greater than the Bohr radius $r > a_0 = 5.29 \cdot 10^{-9}$ cm), we can approximately assume that equation (223) transforms into equation (212).

$$\nabla^2\phi(r) + \frac{4}{3\eta_r^2}\left(\varepsilon + \frac{v_e^2 r_{eff}}{2r}\right)\phi(r) = 0, \tag{226}$$

but the effects associated with the fine structure of the hydrogen atom are not taken into account by this stochastic equation.

CONCLUSION

This fourteenth part of the project, entitled "Geometrized Vacuum Physics (GVP) Based on the Algebra of Signature (SA)" (abbreviated GVPh&AS) [1,2,3,4,5,6,7,8,9,10,11,12,13 or https://metraphysics.ru/], examines the stochastic metric-dynamic model (SMDM) of the "hydrogen atom" as a stable vacuum structure. Using this very simple "atom" as an example, we demonstrate a method for studying its internal structure, which can be applied to constructing SMDM for all known atoms and molecules.

In the framework of the GVPh&AS, a "hydrogen atom" is a stable neutral (i.e., on average, flat) vacuum formation consisting of an "electron" (or yellow e_y^+-"quark") (11) and a "proton", which can have three possible signature (i.e., topological) configurations (31) – (33) with equal probability, and continuously chaotically transform into each other. One of the variants of the metric-dynamic configuration of the "hydrogen atom" is presented in expanded form (72).

Contrary to current concepts, the GVPh&AS predicts the possible existence of a second modification of the "hydrogen atom," consisting of a "positron" (or $e_{ж}^{-}$-"quark") (21) and an "antiproton," which, with varying probability, can have three possible signature (i.e., topological) configurations (34) – (36), continuously and chaotically transforming into each other.

This second variant can be called an "anti-hydrogen atom," but both of these modifications of the "atom" coexist (i.e., they do not annihilate due to continuous topological metamorphoses and constant thermal motion), so it is more correct to call them male and female individuals of the same chemical element. From a spectroscopic perspective, these individuals ("M-hydrogen atom" and "Y-hydrogen atom") are indistinguishable, as they are structured in exactly the same way, being negative copies of each other. In this article, only the "M-hydrogen atom" is considered, as The "hydrogen atom" is structured exactly the same, only turned inside out.

When averaging the set of metrics (72), the core of this “atom” with an effective radius $r_{eff}{\sim}10^{-13}$ cm (see Figure 7a) and a tiny internal nucleolus of the “electron” (i.e., the nucleolus of the e_{y}^{+}-“proto-quark”) with a radius $r_7{\sim}10^{-24}$ cm (see the hierarchy of radii (62) and Figure 11) are distinguished from the chaotically fluctuating vacuum in the vicinity of the center of the “hydrogen atom”

$r_{7eff}{\sim}\mathbf{10^{-17}}\boldsymbol{cm}$

Fig. 11: Fractal illustration of how the outer shell of the e_{y}^{+}-"proto-quark" surrounds its tiny nucleolus (ePQN) with an estimated radius of $r_7{\sim}10^{-24}$ cm, and how the cyclone is entrained by its chaotic motion. At the same time, the part of the outer shell closest to the nucleolus is partly included in the effective size of the ePQN itself, $r_{7eff}{\sim}10^{-17}$ cm (see Figure 7), and influences the magnitude of the main characteristics of the random process being studied, $2\sigma_r^2/\tau_{rcor}$

Let us note again that we have no experimentally confirmed size of the e_y^+-"proto-quark's" nucleolus, but we can confidently state that $r_7 \ll 10^{-17}$*cm.*

In the core of a "hydrogen atom," when averaged, interconnected nucleoli of one d_i^+-"proto-quark" and two u_j^--"proto-anti-quarks" appear (see Figures 6 and 7), which constantly move chaotically relative to the center of the core and relative to each other, and also constantly rearrange topologically into various node combinations (31) – (33) (see Figure 6).

On average, the outer shells of the d_i^+-"proto-quark" and two u_j^--"proto-antiquarks" together form the outer shell of the "hydrogen atom's" core with an effective radius $r_{eff} \sim 10^{-13}$ cm, which, on average, attracts the nucleolus of the e_y^+-"proto-quark" (ePQN), if it is located at a sufficiently large distance from this nucleus ($r \gg 10^{-13}$ cm). This averaged interaction of the "hydrogen atom's" core with the ePQN is of a Coulomb nature and is determined by a potentiality of the form (211)

$$u(r) = -\frac{v_e^2 r_{eff}}{2r}.$$

However, as the ePQN approaches the core of the "hydrogen atom" (i.e., at $r \approx r_{eff}$), it begins to be influenced by the repulsion from the outer shell of the similarly charged d_i^+-"proto-quark". It is proposed to take this circumstance into account by introducing effective potentiality (221)

$$u_{\mathrm{eff}}(r) = -\frac{v_e^2}{2}\arcsin\left(\frac{r_{eff}}{r}\right).$$

The averaged behavior of a chaotically wandering particle (in particular, a ePQN) in a region of space where it is subjected to a constant averaged force (in particular, in the vicinity of the "atom's" core) was considered in [13,14]. These papers demonstrated that the averaged states of such particles are described by the stochastic Schrödinger equation (201).

Taking into account the potentiality (211), the stochastic Schrödinger equation for the considered case of chaotic behavior of a ePQN in the vicinity of the "hydrogen atom's" core has the form (212)

$$\left[-\frac{3\eta_r^2}{4}\nabla^2 - \frac{v_e^2 r_{eff}}{2r}\right]\phi(r) = \varepsilon\phi(r). \qquad (212')$$

This equation coincides, up to constant coefficients, with the quantum-mechanical Schrödinger equation for an electron in a hydrogen atom (213).

The solutions of equations (212) and (213) are identical (217) – (218) up to constant coefficients, and the sought-after functions $\phi(r)$ and $\psi(r)$ have the same value – the probability amplitudes of detecting a chaotically (randomly) wandering particle at a given point in space. However, the interpretations of the stochastic and quantum mechanical approaches and the results obtained are completely different. We will not repeat the Copenhagen interpretation of quantum mechanics (QM) here, as it is widely known. Within the stochastic approach to quantum mechanics, developed in the work of Edward Nelson, the chaotically wandering particle (in particular, the e_y^+-"proto-quark's" nucleolus (ePQN)) has very small dimensions compared to the region of space being studied (in particular, the nucleolus radius is $r_7 \sim 10^{-24}$ cm) and a real trajectory of motion, but it is very complex. Therefore, it is not the ePQN motion itself that is studied, but its average state [13,14].

For example, if we film a bird in a cage for several days and then play back the entire recording for 15 minutes, we won't see the bird, only a blurry spot corresponding to the probability density function of its possible location. Moreover, if we change the conditions of the bird's existence in the cage, for example, by significantly altering the temperature or turning on the light in the room containing the cage and then repeat the same actions with the film recording, we'll find that the configuration of the blurry spot will change abruptly.

In stochastic quantum mechanics, there is no difference between analogous processes in the micro- and macro-worlds. All bodies in a closed region with constant total mechanical energy behave identically, on average, whether it be the nucleus of an e_y^+-"proto-quark" near the core of a "hydrogen atom", a fish in a round aquarium, the chaotically wandering center of mass of a planet, or the trembling nucleus of a living biological cell, etc.

All such random processes obey the same laws, which are determined by the simultaneous influence of two initial principles: the "principle of least action" (leading to the establishment of order in any stochastic system in order to minimize energy and information costs) and the "principle of maximum entropy" (encouraging the stochastic system to fill all its possible states with the most efficient redistribution of energy, which is often accompanied by an increase in chaos).

In the articles [13, 14], both of these principles are combined into a single principle of "extremum efficiency" for any stochastic system (i.e., essentially, for any entity in the world around us, since everything that surrounds us has both a deterministic (i.e., averaged) and a random component of existence). The application of this unifying principle to the study of various stochastic systems, using the calculus of variations, made it possible to obtain stochastic equations for describing the average state of many random processes, including the stochastic Schrödinger equations.

The main difference between quantum mechanical equations and stochastic Schrödinger equations is that instead of the highly limiting application of the ratio of Planck's constant to the particle mass ($\hbar/m_e$), stochastic equations use the ratio of twice the variance of a random process to its autocorrelation coefficient ($2\sigma_r^2/\tau_{rcor}$), which can be estimated for virtually any random process.

It should be noted, however, that in the problem under consideration of studying the averaged behavior of the ePQN in the vicinity of the "hydrogen atom's" core, a geometric aspect is added. Within the framework of the geometrized vacuum physics developed here, there is an outer shell around the e_y^+-"proto-quark's" nucleolus (ePQN), which is a curvature of the vacuum extension surrounding this nucleolus (see §2 in [7]). In the stochastic approach, we practically do not take into account the behavior of the outer shell of the ePQN (see Figures 1, 7d, 11). More precisely, we assume that the distortions and stresses of this outer shell affect the ratio $2\sigma_r^2/\tau_{rcor}$ for a chaotically wandering ePQN. However, upon closer examination, we discover that the outer shell follows the ePQN (see Figure 12) and adopts a certain average topological configuration, depending on the probability density distribution of the ePQN 's location in the vicinity of the "hydrogen atom" nucleus. This average topological configuration of the ePQN 's outer shell can also, in part, be interpreted as the average shape of the electron cloud.

Quantum mechanics in the Copenhagen interpretation practically prohibits insight into the geometric and dynamic structure of intra-atomic processes. Meanwhile, the GVPh&AS [3,4,5,6,7,9,10] in conjunction with stochastic quantum mechanics [13, 14] allows for the formation of metric-dynamic stochastic models of stable vacuum entities, such as the "hydrogen atom," and many other similar geometric-stochastic systems involving chaotically wandering centers, such as other "atoms," the nuclei of biological cells, the centers of mass of planets, stars, galaxies, etc.

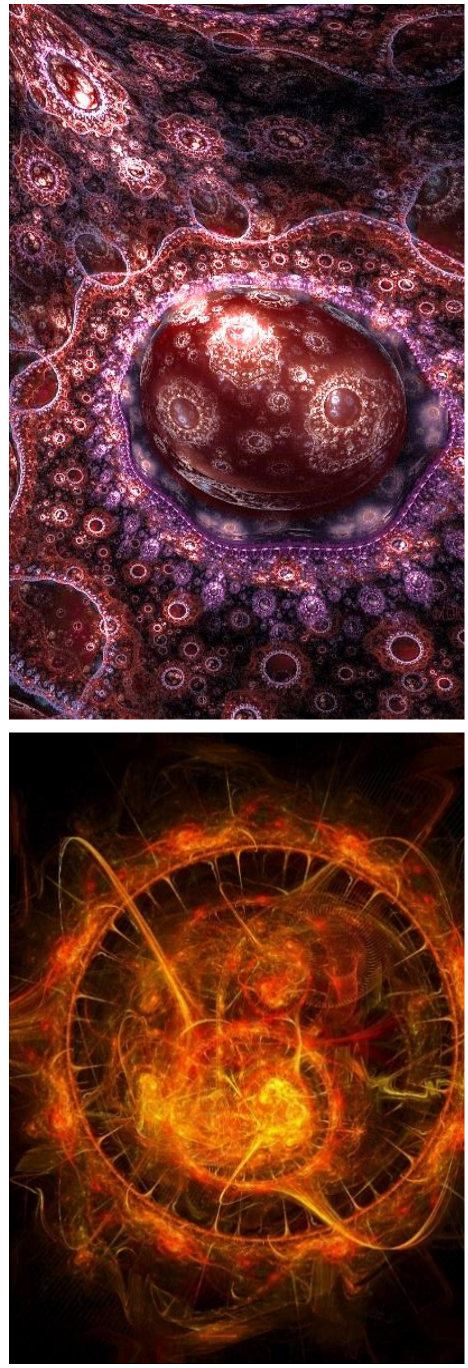

Fig. 12: Fractal illustrations of the seething core of the "hydrogen atom" and the fuzzy outer shell of a chaotically wandering nucleolus of a e_y^+-"proto-quark"

Stochastic equation (212) and the quantum-mechanical Schrödinger equation (213) have the same solutions (217) up to constant coefficients. As a result, they describe the same emission spectra of the hydrogen atom. However, this article proposes modifying the Schrödinger equation for the "hydrogen atom" to take into account the effective potentiality (221). In this case, the stochastic Schrödinger equation has the form (223)

$$\nabla^2\phi(r)+\frac{4}{3\eta_r^2}\left[\varepsilon+\frac{v_e^2}{2}\arcsin\left(\frac{r_{eff}}{r}\right)\right]\phi(r)=0. \qquad (223')$$

Potentialities (211) and (221) are very similar, especially at large distances from the "atom's" core (see the graphs in Fig. 10). However, small deviations of Eq. (223) from Eq. (212) may help refine the "hydrogen atom" emission spectrum and align it with experimental data without radiative corrections.

The method presented in this article for identifying a stochastic metric-dynamic model of the "hydrogen atom," based on averaging a set of metric solutions to Einstein's vacuum equation (72), can be applied to construct similar models of any "atoms" from D.I. Mendeleev's periodic table of chemical elements. For example, one of many possible topological (nodal) configurations of the ^4He-"helium atom" is presented below.

$$\begin{array}{rl}
\begin{array}{c}(+\ +\ -\ +)\\(-\ -\ +\ +)\\(-\ +\ +\ -)\end{array} & p_2^{-}\text{-«протон»} \\[6pt]
\begin{array}{c}(-\ +\ -\ -)\\(+\ -\ -\ +)\\(+\ -\ +\ -)\end{array} & p_3^{+}\text{-«антипротон»} \\[6pt]
(-\ +\ +\ +) & \text{«позитрон»} \\[6pt]
\begin{array}{c}(-\ -\ -\ -)\\(+\ +\ -\ +)\\(+\ +\ +\ -)\\(-\ -\ +\ +)\end{array} & n_2^{0}\text{-«нейтрон»} \\[6pt]
\begin{array}{c}(+\ +\ +\ +)\\(+\ -\ +\ -)\\(-\ +\ -\ -)\\(-\ -\ -\ +)\end{array} & n_6^{0}\text{-«нейтрон»} \\[6pt]
(+\ -\ -\ -) & \text{«электрон»} \\
\hline
{}^4He\ (0\ \ 0\ \ 0\ \ 0) & \text{«атом гелия»}
\end{array} \qquad (227)$$

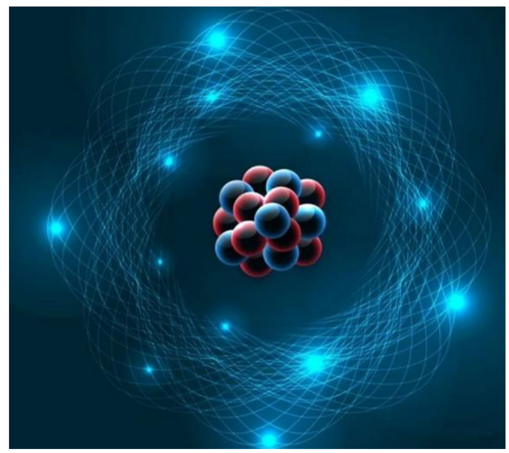

where each signature in the numerator of the rank (227) corresponds to a “quark” or “antiquark” from the Table 1, which are specified by sets of 10 metrics of the form (2) – (10).

A probabilistic approach to metric solutions to einstein's vacuum equations

In this article, as in the entire GVF&AS project [1,2,3,4,5,6,7,8,9,10,11,12,13] or https://metraphysics.ru/], we assumed that all metric solutions to Einstein's vacuum equation relate to the metric-dynamic system they describe with equal probability. For example, within the GVPh&AS framework, the metric-dynamic model of the "proton's" outer shell is described by a set of 12 metric solutions (40), (43), and (46) to Einstein's second vacuum equation. In this averaging, we assumed that each of these metric solutions can appear in the overall system with an equal probability of 1/12.

However, if we assume that all these metric solutions can manifest themselves in the system (i.e. in the “corpuscle”) with different probabilities, then the mathematical apparatus of the GVPh&AS will become incomparably richer and will possibly allow us to describe a significantly wider class of phenomena.

The place of quantum field theory and associative physics in modern scientific paradigms

There are several dominant approaches in modern science:

1) Quantum field theory (QFT) is a fundamental branch of physics that combines the principles of quantum mechanics and special relativity. It describes the behavior of elementary particles and their interactions not as the motion of point objects, but as excitations (quanta) of fundamental fields permeating spacetime. Within this theory:
- classical fields (electromagnetic, Dirac fields) become operators acting on states;
- processes appear identical to all inertial observers (i.e., Lorentz invariance holds);
- according to Emmy Noether's theorem, every continuous symmetry of the Lagrangian field generates conserved current and charge (energy, momentum, electric charge, color charge, etc.);
- the interactions of fields and their quanta occur at a single point in spacetime. This avoids "action at a distance" (locality).
Unlike conventional quantum mechanics, where a particle is a wave packet and describes systems with a fixed number of particles, quantum field theory (QFT) postulates that the fundamental entity is a field filling all of spacetime. In QFT, an electron is not a point-like sphere, but a quantum of excitation of an electron-positron field, while a photon is a quantum of excitation of an electromagnetic field. Thus, particles are ripples or quanta (the smallest portions of energy) of their fields. The number of particles is not constant. They can be created and disappear (annihilate), transforming into other fields. For example, an electron + positron → two photons.
The main problems of QFT:
- in QFT, calculations often yield infinite values for physical quantities (e.g., the mass and charge of particles). This is due to the fact that spacetime in the theory is considered continuous and infinitely divisible, and quantum fluctuations on arbitrarily small scales lead to mathematical ultraviolet divergences.
- QFT cannot be reconciled with general relativity. Attempts to apply QFT methods to the gravitational field lead to irreconcilable mathematical contradictions and divergences.
- In QFT, the vacuum is not a void, but a state of fields with minimal energy, filled with quantum fluctuations. This leads to difficulties in interpreting physical processes and to the emergence of so-called "virtual particles," which are not directly observable but influence calculations.
- Despite its rigorous mathematical formulation, axiomatic quantum field theory (QFT) fails to construct a consistent theory of interacting fields or derive new experimentally verifiable consequences, other than the spin-statistics theorem and the CPT theorem.
- In some cases, experimental data (e.g., the anomalous magnetic moment of the muon) show deviations from QFT predictions, which may indicate the theory's incompleteness.
- QFT methods (e.g., perturbation theory, Feynman diagrams) are very complex and do not always yield exact solutions for interacting fields. Most results are obtained only as approximations.

2) General Relativity (GR) is a theory in which massive bodies and energy curve a unified space-time continuum. Space-time ceases to be a formal stage against which force interactions between material bodies play out. It itself becomes a participant in these processes. Bodies not only curve space-time but also move along its geodesics, i.e., along the shortest paths in this four-dimensional curved continuum. The main tool of general relativity is the Einstein-Hilbert equation for finding the metric in each local region of spacetime

$$R_{\mu\nu} - \frac{1}{2} R g_{\mu\nu} = \frac{8\pi G}{c^4} T_{\mu\nu}$$

and the Einstein equation with the lambda term

$$R_{\mu\nu} - \frac{1}{2} R g_{\mu\nu} + \Lambda g_{\mu\nu} = \frac{8\pi G}{c^4} T_{\mu\nu}$$

where $R_{\mu\nu} - \frac{1}{2} R g_{\mu\nu} = G_{\mu\nu}$ (the Einstein tensor) describes the curvature of spacetime;
$T_{\mu\nu}$ (the energy-momentum tensor) describes matter and energy;
Λ is the cosmological constant (the lambda term).
John Wheeler commented on this equation as follows: "Matter tells spacetime how to curve, and spacetime tells matter how to move."
General relativity underlies modern cosmological theories (it describes the expansion of the Universe) and is used to construct navigation systems like GPS. General relativity predicted the existence of black holes, gravitational waves, and gravitational lensing, and explained a number of effects, such as the additional shift in the perihelion of the orbits of planets in the Solar

System; the bending of light in the gravitational field of a star; and the redshift of light when leaving the strong gravitational field of cosmic bodies.
The main shortcomings of general relativity are:
- this theory retains massive bodies, which cannot be geometrized;
- it is unclear how bodies curve spacetime;
- curved space and time are not physically determinable, as these abstract concepts cannot be directly measured;
- Inside a black hole (at the center) and at the moment of the Big Bang, general relativity predicts infinite quantities (singularities). This means the theory is incomplete.
- General relativity doesn't work in the microworld. Elementary particles, atoms, and molecules don't obey it;
- General relativity doesn't unify with quantum field theory or quantum field theory. The quantum theory of gravity has not yet been completed.

3) String theory (or superstrings) (ST) is a branch of theoretical physics that attempts to unite the general theory of relativity (gravity, describing the macroworld) and quantum field theory (description of the microworld), i.e., it attempts to create a "Theory of Everything." In this theory, the basic objects are one-dimensional "strings" (loops or threads) in a 10 (or 11)-dimensional space with a Punk length of ~ 10^{-33} cm. Different frequencies (vibrational modes, notes) of superstring vibrations generate different particles. One note = photon, another note = electron, a third note = gluon, etc., including a note = graviton. The vibrational modes of the strings determine the masses, charges, and other characteristics of elementary particles. String theorists distinguish between closed strings (loops) that generate gravitons and open strings (threads) whose ends are attached to multidimensional D-branes (from the English membrane). The theory is based on the principle of supersymmetry, which assumes the existence of symmetry between bosons and fermions. This allows us to eliminate a number of mathematical contradictions and incorporate gravity into quantum theory. The main drawbacks of the String theory are: 1) to observe superstrings, an energy of about ~ 10^{19} GeV is required, which is 10 quadrillion times higher than the capabilities of the Large Hadron Collider (LHC); 2) in the SSTS, there are ~ 10^{500} possible vacuum variants, and it is not clear how to identify the true vacuum from them; 3) the abstract nature of the extremely complex mathematical apparatus of the String theory.

4) Loop Quantum Gravity (LQG) is the second leading candidate for a theory of quantum gravity that unites Einstein's general relativity and quantum mechanics. Unlike superstring theory, LQG does not introduce extra dimensions or hypothetical objects (strings), but attempts to directly quantize spacetime itself. LQG assumes that space is not divisible to infinity, but to minimal volumes of the order of ~ 10^{-99} cm^3. At these scales, space looks like foam, or like a fabric (a 3-dimensional spin network) woven from loops. The spin network in LQG is a graph (with knots and lines connecting them). The knots represent volume quanta, and the lines represent area quanta. If time (evolution) is added to this network, the network lines smear into a 4D surface resembling foam. Quantum excitations of the gravitational field propagate through the spin network. In classical general relativity, at the beginning of the Big Bang and at the center of a black hole, the density of matter becomes infinite. However, LQG suggests that the compression stops at a minimum volume, and a "Big Bounce" occurs. In this case, the black hole could transform into a new Universe. Thus, LQG allows us to consider scenarios of a pulsating Universe, where the Big Bang could be a "Big Bounce", i.e., a transition from compression to expansion of the Universe. This opens new horizons for cosmology and understanding the early Universe. Since space is discrete in LQG, there are no infinitesimal distances, and therefore there are no infinities in quantum calculations. The LQG equations can be written without time (i.e., time is not fundamental—this is called the "time problem" in quantum gravity). Instead of positing gravity as an exchange of particles (gravitons, as in string theory), LQG utilizes the principles of holography and gauge invariance. The key variable is the area operator, which has a discrete spectrum of eigenvalues. Unlike many other quantum field theories, LQG does not assume the existence of a fixed spacetime as an arena for physical processes. Spacetime itself becomes a dynamic variable, emerging from quantum states. A key step was the use of Ashtekar variables, which allowed the application of quantum theory methods to the geometry of spacetime. Unlike string theory, LQG makes specific (though still untested) predictions:
- Lorentz invariance may be violated on small scales: The speed of photons in a vacuum may depend slightly on their energy (the "flickering light" effect). Satellites (e.g., GLAST/Fermi) are searching for such effects;
- LQG predicts that black holes can evaporate due to Hawking radiation, leaving a "Planck-sized remnant" rather than a singularity.
- LQG predicts small deviations from the thermal spectrum of Hawking radiation, which are theoretically detectable but very difficult.
The main problems with LQG are:
- it is unclear how to obtain smooth Einstein spacetime (the classical limit) from quantum "foam."

- in this theory, pure gravity is easily quantized, but the addition of matter particles (electrons, quarks) to the theory still seems unnatural;
- it uses extremely complex mathematics (SU(2) group, Ashtekar constraints), so a rigorous proof of the consistency of LQG is incomplete;
- it is not entirely clear how all known physical fields arise in LQG;
- experimental confirmation of LQG predictions is associated with high energy costs and technical difficulties.

5) Etherodynamics is a marginal direction in modern physics, based on the concept of the existence of the original, all-pervading material medium - ether (consisting of extremely small particles - amers). Supporters of this direction assume that the mechanical ether has a non-zero mass density, properties of an ideal gas and / or liquid. They claim that etherodynamics, based on the equations of gas and hydrodynamics, allows us to abandon abstract and non-obvious (neopositivistic) concepts and postulates of the theory of relativity and quantum theories, and return physics to "visual images" and "common sense". Within the framework of etherodynamics, elementary particles (electrons, protons, neutrons, etc.) are stable vortex structures of ether (toroidal vortices). Electric charge is the result of rotation of ether vortices; electric field is the movement of ether in the form of conical tubes; A magnetic field is the organized movement of ether along the axis of vortices, forming magnetic domains; gravity is a consequence of a local decrease in etheric pressure between massive bodies, leading to their attraction; light and electromagnetic waves are waves in the ether, propagating at a finite speed determined by the properties of the ether (its density, viscosity, etc.). Proponents of etherodynamics believe that its development could lead to new energy sources and technologies.
The main shortcomings of etherodynamics:
- amers (ether particles) have not been experimentally detected; Critics point out that etherodynamics as a whole has not provided reproducible experimental evidence for the existence of ether;
- the mathematical apparatus of gas and hydrodynamics is limited, i.e., unsuitable (or rather, poor) for describing many observed phenomena.

This theory is viewed critically in academic circles. There is an "unspoken ban" on such research in the scientific community. At the same time, a number of conventional scientists note that, despite the lack of indisputable experimental evidence of the existence of ether, the search for alternative theories (including etheric ones) is useful in times of crisis in he "Geometrized Vacuum Physics Based on the Algebra of Signature" (GVPh&AS) developed here [1,2,3,4,5,6,7, 8,9,10,11,12,13] to some extent unites (or rather, incorporates) all of the above-mentioned leading directions in physics.

1] In GVPh&AS, "corpuscular"* metric-dynamic models of virtually all "elementary particles" were obtained in almost complete agreement with the elements of the Standard Model of elementary particles (see §4 in [7]). It should be noted, however, that GVPh&AS has one more i_w^{+}-"quark" and one more i_w^{-}-"antiquark" than the Standard Model. In addition, the movements of any nuclei of "corpuscles" have a random component, which is described by stochastic differential equations and, in particular, the Schrödinger equations [6,13].

The vacuum is quantized into an infinite number of nested $\lambda_{m,n}$-vacuums (see [1]) (this is a longitudinal quantization of the vacuum) and, in turn, each $\lambda_{m,n}$-vacuum is stratified (quantized) into an infinite number of metric extensions with 16 possible signatures (see [2]) (this is a transverse quantization of the vacuum). Thus, GVPh&AS has much in common with quantum field theory (QFT) and with quantum mechanics (QM).

2] The GVPh&AS is a modernization of General Relativity, in which Einstein's vacuum equations are considered as conservation laws for, on average, stable vacuum formations. An infinite number of $\pm\Lambda_i$-terms are added to these equations, and the vacuum is also considered as the intersection of 16 metric 4-dimensional subspaces with 16 types of signatures (60). These fundamental additions to General Relativity make it possible to construct the Hierarchical Cosmological Model [6]. Thus, the HVF&AC is a direct continuation of Einstein's General Relativity.

3] The GVPh&AS is based on the superposition (additive and/or multiplicative superposition) of 4-dimensional metric spaces with 16 possible signatures (i.e., topologies) (60). Together, these spaces form a Ricci null space, a flat space that has much in common with a Calabi-Yau manifold (see [15]). Each metric space has 4 dimensions, so if we consider a superposition of 16 spaces with signatures (60), the total number of dimensions is 16 × 4 = 64, but they collapse harmonically to 2 × 4 = 8 dimensions. Thus, the GVPh&AS can be unwound as a multidimensional theory that has much in common with superstring theory.

It should be noted, however, that there are no additional dimensions in the GVPh&AS. The fact is that the GVPh&AS is simply an extended version of elasticity theory (a more accurate one), where instead of one curved tri-basis, 8 internal and 8 external distorted 3-sided angles of one curved cube of a continuous medium (in particular) a vacuum are considered at once (see [1,2]). That is, instead of a strain tensor with 9 components in elasticity theory, in the GVPh&AS the curvature of a local region of a continuous medium (in particular, a vacuum) is described by 256 components of a metric tensor, from which its various characteristics are obtained: deformations, torsion, curvature, velocities and accelerations of displacement and rotation, etc. (see [1,2,3,4]).

4] In Loop Quantum Gravity (LQG), there is a minimal indivisible volume of 3-dimensional space (vacuum (of the order of ~ 10^{-99} cm^3), and in GVPh&AS there is a "corpuscle" ("instanton") with a minimal core with a radius of the order of r_{1m} ~ 10^{-55} cm (i.e., with a volume of ~ 10^{-165} cm^3). As has been noted many times, within GVPh&AS, we do not know which core in the hierarchical chain (62) is the smallest (see [6]), since it is far beyond the observational limit. But such a minimal core in GVPh&AS must exist, otherwise this theory loses its support and closure. It is possible that the minimal core is the core of plankton from the hierarchy (62) with an approximate radius of the order of r_{8m} ~ 10^{-34} cm (i.e., with a volume of ~ 10^{-100} cm^3). In In this case, the GVPh&AS and the LQG will have even greater similarities. However, there is also a significant discrepancy: when gravitational compression reaches the Planck volume of ~ 10^{-99} cm^3, the LQG predicts a rebound leading to the creation of a new Universe, while in the GVPh&AS, the largest closed mega-Universe is located inside the smallest core in the hierarchical chain (62) (this is the "instanton" core, see §3 in [6]).

5] When treating the world around us as an objective physical reality (i.e., when solving applied problems), in the GVPh&AS it is permissible to consider the illusory space-time continuum (i.e., Einstein's vacuum) as an elastic-plastic medium in which any deformation is inevitably accompanied by the emergence of intertwined intra-vacuum flows (see Figure 3a). In this case, the stratified vacuum as a hypothetical continuous medium conditionally potentially possesses the properties of a gas, liquid, and solid. Such a vacuum in many respects coincides with the mechanical world ether in properties, but with zero averaged characteristics. Einstein's vacuum equations, under certain conditions and simplifications, are reduced to the equations of hydro- and gas dynamics. For example, for small perturbations of the vacuum extent, the first vacuum equation $R_{ik} = 0$ is reduced to the wave equation [16]. Moreover, GVPh&AS, like etherodynamics, attempts to use stochastic geometrized mathematics not only to predict experimental results (a neopositivistic approach), but also to construct images of stable vacuum entities ("quarks," "elementary particles," "atoms," "molecules" of various scales). GVPh&AS also attempts to discern the contours of intranuclear processes. In other words, GVPh&AS, like etherodynamics, attempts to construct a visual (figurative) physics rather than abstract constructs of operators over aggregates in Hilbert space based on the Lagrangian formalism. Even the images generated by the mathematical apparatuses of GVPh&AS and etherodynamics largely coincide. For example, in etherodynamics, moving elementary particles are represented in the form of toroidal vortices of ether; similarly, in GVPh&AS, moving "corpuscles" are toroidal-helical vortices induced in a vacuum around their nuclei (see [8]).

Thus, "Geometrized Vacuum Physics Based on the Algebra of Signature" (GVPh&AS) to one degree or another includes the basic postulates and ideas of all the main theoretical concepts about the physical reality that surrounds us: quantum mechanics (QM), quantum field theory (QFT), general theory of relativity (GTR), loop quantum gravity (LQG) and Etherodynamics (ED).

It should also be noted that the GVPh&AS is an attempt to combine the concepts of ancient Jewish, Arabic, Christian, Chinese, Indian, Greek, Egyptian, and Zoroastrian (Persian) views on the structure of the Universe. In particular, the Algebra of Signatures and the Light-Geometry of the Vacuum are based on the Algorithms of Revealing the Great and Strictly Name of the ALMIGHTY י-ה-ו-ה (Yud-Key-Vav-Key, H'VHI,) (TETRAGRAMMATON) and the teaching about the World from the Void. The great sages of previous generations labored for us and left us the Greatest Heritage. We must simply realize that the ancient sages were closer to the Sources of the Universe; they saw further and deeper than us.

ACKNOWLEDGEMENTS

I sincerely thank Gavriel Davidov, David Reid, Tatyana Levy, David Kogan, Gennady Ivanovich Shipov, Evgeny Alekseevich Gubarev, Carlos J. Rojas, Alexander Maslov, Alexander Bolotov and Georgy Usachev for their assistance.

REFERENCES

[1] Batanov-Gaukhman, M. (2023). Geometrized Vacuum Physics. Part I. Algebra of Stignatures. Avances en Ciencias e Ingeniería, 14 (1), 1-26, https://www.executivebs.org/publishing.cl/avances-en-ciencias-e-ingenieria-vol-14-nro-1-ano-2023-articulo-1/ ; and Preprints, 2023060765. https://doi.org/10.20944/preprints202306.0765.v3, or viXra:2403.0035.

[2] Batanov-Gaukhman, M. (2023).Geometrized Vacuum Physics. Part II. Algebra of Signatures. Avances en Ciencias e Ingeniería, 14 (1), 27-55, https://www.executivebs.org/publishing.cl/avances-en-ciencias-e-ingenieria-vol-14-nro-1-ano-2023-articulo-2/: and Preprints, 2023070716, https://doi.org/10.20944/preprints202307.0716.v1, or viXra:2403.0034.

[3] Batanov-Gaukhman, M. (2023). Geometrized Vacuum Physics. Part III. Curved Vacuum Area. Avances en Ciencias e Ingeniería Vol. 14 nro 2 año 2023 Articulo 5, https://www.executivebs.org/publishing.cl/avances-en-ciencias-e-ingenieria-vol-14-nro-2-ano-2023-articulo-5/; and Preprints 2023, 2023080570. https://doi.org/10.20944/preprints202308.0570.v4, or viXra:2403.0033.

[4] Batanov-Gaukhman, M., (2024). Geometrized Vacuum Physics. Part IV: Dynamics of Vacuum Layers. Avances en Ciencias e Ingeniería Vol. 14 nro 3 año 2023 Articulo 1 https://www.executivebs.org/publishing.cl/avances-en-ciencias-e-ingenieria-vol-14-nro-3-ano-2023-articulo-1/, and Preprints.org. https://doi.org/10.20944/preprints202310.1244.v3, or viXra:2403.0032.

[5] Batanov-Gaukhman, M., (2024). Avances en Ciencias e Ingeniería Vol. 14 nro 3 año 2023 Articulo 2 https://www.executivebs.org/publishing.cl/avances-en-ciencias-e-ingenieria-vol-14-nro-3-ano-2023-articulo-2/, or viXra:2405.0002.

[6] Batanov-Gaukhman, M. (2024) Geometrized Vacuum Physics Part 6: Hierarchical Cosmological Model, Avances en Ciencias e Ingeniería Vol. 14 nro 4 año 2023 https://www.executivebs.org/publishing.cl/avances-en-ciencias-e-ingenieria-vol-14-nro-4-ano-2023-articulo-3/ or viXra:2408.0010.

[7] Batanov-Gaukhman, M. (2025). Geometrized Vacuum Physics Part VII: "Electron" and "Positron", Avances en Ciencias e Ingeniería Vol. 15 nro 1 año 2024 Articulo 3, https://www.executivebs.org/publishing.cl/avances-en-ciencias-e-ingenieria-vol-15-nro-1-ano-2024-articulo-3/, or viXra:2409.0097.

[8] Batanov-Gaukhman, M. (2025) Geometrized Vacuum Physics. Part VIII: Inertial Electromagnetism of Moving «Particles»//Advances en Ciencias e Ingeniería Vol. 15 nro 2 año 2024 Articulo 1, https://www.executivebs.org/publishing.cl/avances-en-ciencias-e-ingenieria-vol-15-nro-2-ano-2024-articulo-1/, or viXra:2411.0086.

[9] Batanov-Gaukhman, M. (2025) Geometrized Vauum Physics. Part IX: «Neutrino»//Avances en Ciencias e Ingeniería Vol. 15 nro 3 año 2024 Articulo 1, https://www.executivebs.org/publishing.cl/avances-en-ciencias-e-ingenieria-vol-15-nro-3-ano-2024-articulo-1/ or viXra:2501.0059

[10] Batanov-Gaukhman, M. (2025) Geometrized Vac-uum Physics. Part X: Naked «Planets» and «Stars»// Avances en Ciencias e Ingeniería Vol. 15 nro 3 año 2024 Articulo 2, https://www.executivebs.org/publishing.cl/avances-en-ciencias-e-ingenieria-vol-15-nro-3-ano-2024-articulo-2/, or viXra:2502.0139.

[11] Batanov-Gaukhman, M. (2025) Geometrized Vacuum Physics. Part XI: Gravity And Levitation //Avances en Ciencias e Ingeniería, Vol. 15 nro 4 año 2024 Articulo 1. Publicada el agosto 7, 2025.https://www.executivebs.org/publishing.cl/avances-en-ciencias-e-ingenieria-vol-15-nro-4-ano-2024-articulo-1/, or viXra:2504.0180.

[12] Batanov-Gaukhman, M. (2025) Geometrized Vacuum Physics. Part XII: Naked "Galaxies" - "Particles" of Dark Matter?//Avances en Ciencia e Ingeniería, Vol. 16 nro 1 año 2025: 1- 46, DOI: 10.65093/aci.v16.n1.2025.21 and viXra:2508.0158.

[13] Batanov-Gaukhman, M. (2025). Geometrized vacuum physics. Part XIII: Connection with quantum mechanics// Avances en Ciencia e Ingeniería, Vol. 16 nro 2: 21–57. https://doi.org/10.65093/aci.v16.n2.2025.28 and viXra:2510.0084

[14] Batanov-Gaukhman M. (2024) Development of the Stochastic Interpretation of Quantum Mechanics by E. Nelson. Derivation of the Schrödinger-Euler-Poisson Equations. *Recent Progress in Materials* **2024**; 6(2): 014; 10.21926/rpm.2402014, or arXiv:2011.09901v10.

[15] Batanov-Gaukhman, M. (2026). Analog of a Compact Calabi-Yau Manifold Based on the Algebra of Signatures. Int J Quantum Technol, 2(1), 01-19, DOI10.66311/3068-9090.02.01.12.

[16] Landau L.D., Lifshitz E.M. (1971) The Classical Theory of Fields / Course of theoretical phys-ics, V. 2 Translated from the Russian by Hamermesh M. University of Minnesota – Pergamon Press Ltd. Oxford, New York, Toronto, Sydney, Braunschwei, p. 387.